SAPIENZA
Università di Roma
Facoltà di Farmacia e Medicina

Ph.D. in
MORPHOGENESIS AND TISSUE ENGINEERING

XXXII Ciclo
(A.A. 2018/2019)

PKCθ as a target to manipulate satellite cell function

Ph.D. Student
Anna Benedetti

Tutor
Prof. Marina Bouchè

Coordinator
Prof. Antonio Musarò

INDEX

SUMMARY

Skeletal muscle regeneration following injury depends on the ability of satellite cells (SCs) to proliferate, differentiate, self-renew, and eventually repair the damage. SC function declines with age and in certain pathological conditions, such as Duchenne Muscular Dystrophy (DMD). Previously we demonstrated that lack or inhibition of Protein kinase Cθ (PKCθ), in a mouse model of DMD (mdx mouse) is associated with a significant improvement in muscle regeneration, which is primarly due to reduced inflammation; hovever, it might also depend on a direct effect on SCs. Therefore, in this study we examined the potential role of PKCθ in SC function. We show that PKCθ is expressed in SCs and its active form is localized to the chromosomes during prophase, to the centrosomes during metaphase and to the midbody during cytokinesis. Interestingly, symmetric division of Pax7+/MyoD- SCs and the number of self-renewing SCs were significantly increased on single myofibers isolated from PKCθ-/- mice compared to wild type, after 2 and 3 days in culture. Genetic ablation of PKCθ or its pharmacological inhibition *in vivo* had no effect on SC number in healthy muscle. By contrast, after induction of muscle injury lack or inhibition of PKCθ resulted in a significant expansion of a population of self-renewing SCs known to contribute to the maintenance of the satellite cell pool. Lack of PKCθ had no effect on SC proliferation *in vitro* and *in vivo* and did not alter the inflammatory milieu after acute injury in muscle. Thus, the enhanced self-renewal ability of SCs in PKCθ-/- mice is not due to an increased proliferation or a different crosstalk between SCs and immune cells. Together, these results suggest that PKCθ absence or inhibition lead to an increased SC self-renewal by stimulating their expansion through symmetric division. In conclusion, PKCθ may be a promising target to manipulate satellite cell self-renewal in pathological conditions.

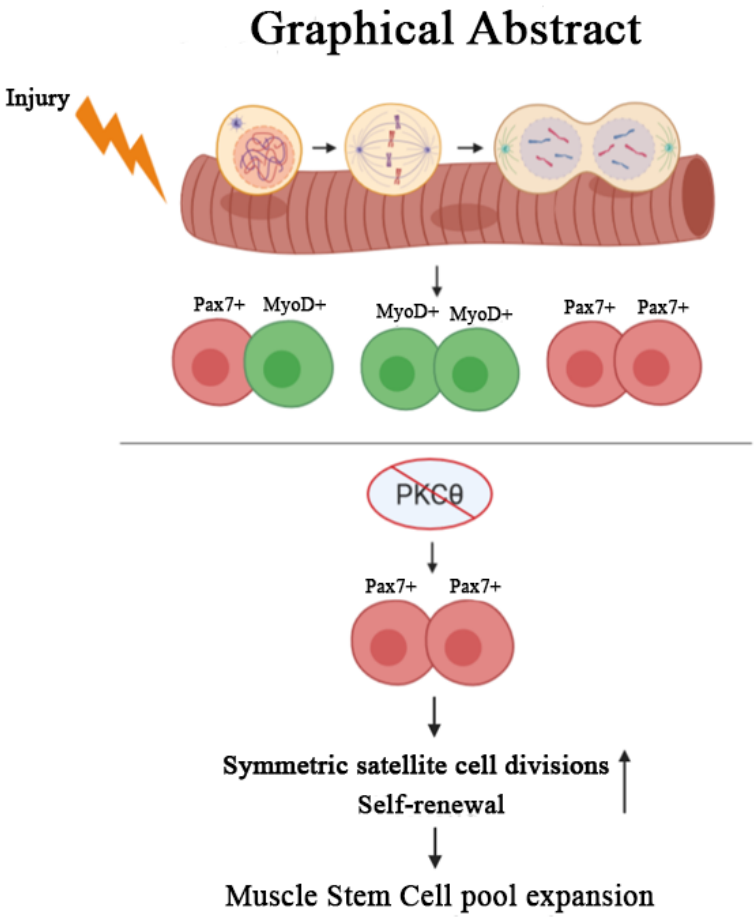
Graphical Abstract
Injury
Pax7+ MyoD+
MyoD+ MyoD+
Pax7+ Pax7+
PKCθ
Pax7+ Pax7+
Symmetric satellite cell divisions
Self-renewal
Muscle Stem Cell pool expansion

1. INTRODUCTION

1.1 Satellite cells and muscle regeneration

1.1.1 Satellite cells in normal and regenerating muscle

Satellite cells (SCs) are the adult stem cells of skeletal muscle, first identified by Mauro [1]. They are so called because of their position between the sarcolemma and the basal lamina of the fiber [1]. During development, satellite cells originate from the dermomyotome, an epithelial structure on the dorsal part of the somites, from progenitor cells expressing the transcription factors Pax7 and Pax3. In the mouse embryo, during day 16.5 to 18.5, progenitor cells migrate to a position between the primitive basal lamina and the myotome. After birth, these cells begin to expand and acquire the adult phenotype [2]. Pax7 is the common biomarker used to identify satellite cells in adult muscle, because quiescent and proliferating satellite cells express it. Other important markers of satellite cells include, among others, M-cadherin, c-Met, α7-integrin, CD34, and syndecan 3 and 4 [3].
Satellite cells have long been considered a homogeneous population of progenitor cells. However, more and more studies support the findings that SCs are a heterogeneous population of cells based on their genetic signature, phenotype as well as stemness and myogenic propensity [4].
Satellite cells are mitotically quiescent (in G_0 phase) under steady state, but following muscle injury they enter the cell cycle, expand and fuse to repair the muscle. At the same time, some of the satellite cells undergo self-renewal, a process necessary for the maintenance of the SC pool [5]. Quiescent SCs show a unique transcriptomic profile, with genes involved in transcriptomic control, negative regulators of cell cycle, cell-cell and cell- ECM adhesion and lipid transporter for metabolic control. At the epigenetic level half of the protein-coding genes show an active chromatin state, acquiring histone H3 Lys4 trimethylation

(H3K4me3). These findings suggest that quiescent SCs are primed for activation, to respond to an injury signal rapidly [6]. One of the key factors promoting SC quiescence is the transmembrane protein Notch. When Notch ligands Delta or Jagged bind to the receptor, the Notch intracellular domain Nicd is cleaved. Nicd then translocates to the nucleus where it interacts with downstream effectors such as recombining binding protein-Jκ (RBPJκ) [7]. RBPJκ and Nicd can bind the Pax7 promoter directly, thereby inducing its expression. Furthermore, Hes and Hey, two of the Notch target genes, reduce Myod mRNA, one of the main myogenic regulatory factors [8].
After muscle injury SCs are exposed to external stimuli that induce their activation, and cause a profound epigenetic transformation. Activated satellite cells express genes involved in cell cycle entry and progression, chemotaxis, and metabolic processes [9]. After activation, satellite cells start to express other myogenic factors such as Myf5 and MyoD, and enter cell cycle by 24-48h after injury. Activated satellite cells also start to migrate to reach the site of injury [5]. These cells can migrate along the same myofiber, or they can also migrate to other myofibers, by crossing the basal lamina [10].
MyoD is an important regulator of satellite cell differentiation. In the absence of MyoD, satellite cells do not differentiate and remain mostly in the proliferative state, with propensity for self-renewal [11].
After the proliferative phase, SCs enter the myogenic program and begin to fuse together or with preexisting fibers. The transcription factors regulating the switch from proliferation to differentiation are Myf6 (aka Mrf4), Mef2, and myogenin, which is mainly induced by MyoD [12]. These are master regulators that induce muscle-specific genes, such as myosin, actin and troponin. The transcriptional activity of these master transcription factors can be regulated at the post-transcriptional level: p38 α/β has been shown to phosphorylate and activate Mef2 and MyoD, stimulating their binding to promoters [13]. HDACs can either directly inhibit

MyoD transcriptional activity [14], or indirectly through a Mef2-dependent pathway [15].
Micro RNAs, have also been shown to regulate myogenic differentiation. MRFs induce the expression of microRNAs such as miR-1, miR-133 and miR-206, which regulate the expression of myogenic genes [16].

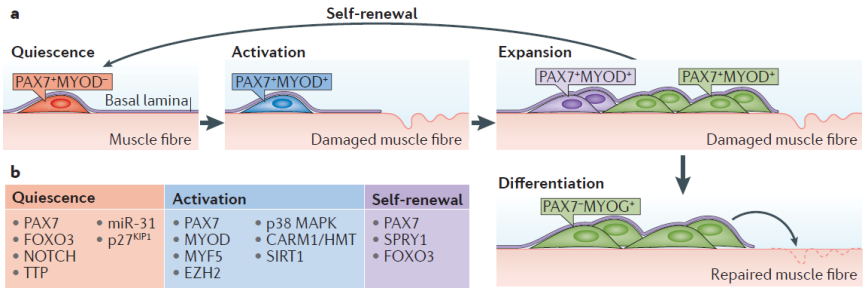

.E. Almada and A.J. Wagers, Mol Cell Biol (2016).

Figure 1: a: recapitulation of satellite cell activation and differentiation mechanism; b: Intrinsic factors expressed in quiescent, activated and self-renewing cells.

The process of myoblast fusion is regulated by different intracellular or membrane-bound proteins, such as β1-integrin, VLA-4 integrin, the receptor VCAM, and caveolin-3. These proteins promote cell recognition and adhesion. A first phase of myoblast fusion (primary fusion) forms small myotubes. Then, a second myoblast fusion wave incorporates new myoblasts to the nascent myofiber, thereby completing the myofiber growth. Newly formed myofibers can be recognized by their small size compared to normal fibers, by the centrally located nuclei, and the by expression of embryonic Myosin Heavy Chain (eMHC). With the progression of muscle regeneration, these fibers increase in size, the nuclei move to the periphery, and the muscle is fully regenerated by day 50 after injury [5].

1.1.2 Satellite cell self-renewal

As previously mentioned, like other adult stem cells, satellite cells are also able to self-renew, to maintain the muscle stem cell pool throughout life. Self-renewal can be achieved by symmetric or asymmetric division. In the first case a single cell gives rise to two identical cells that will both differentiate or go back to quiescence. In the asymmetric division, a cell generates two cells, one of which will differentiate and the other will self-renew [5]. Satellite cell ability to self renew was demonstrated with single myofiber transplantation experiments in scid-mdx (immunodeficient and dystrophic) mice. It was found that myofiber associated satellite cells after engraftment could undergo 10 fold expansion via self-renewal [17]. In addition experiments of single SC transplantation in scid-mdx mice, showed that transplanted SC could form new myofibers and also migrate to the quiescent niche [18]. Rudnicki's group demonstrated that the choice of SCs to undergo symmetric or asymmetric self-renewal, depends on the mitotic spindle orientation relative to the myofiber axix. Experiments conducted with *Myf5Cre;R26R-loxP-stop-loxP-YFP* mice, showed that asymmetric division is predominantly perpendicular to the myofiber axis. It gives rise to one SC 'stem' cell (Pax7+/Myf5-) that remains anchored to the basal lamina, and one cell (Pax7+/Myf5+) adjacent to the myofiber that will differentiate. Symmetric division happens when the mitotic spindle is parallel to the myofiber and can generate Pax7+/Myf5- or Pax7+/Myf5+ cells [19]. The Pax7+/Myf5- symmetric division is promoted by Wnt7a, or by the inhibition of JAK-STAT pathway during muscle regeneration [20], [21]. Pax7+/Myf5- SCs represent 10% of the total population of SCs. They are considered the true stem cells, because when transplanted into Pax7-/- mice they can reconstitute the stem cell compartment much more efficiently than Pax7+/Myf5+ cells [19].

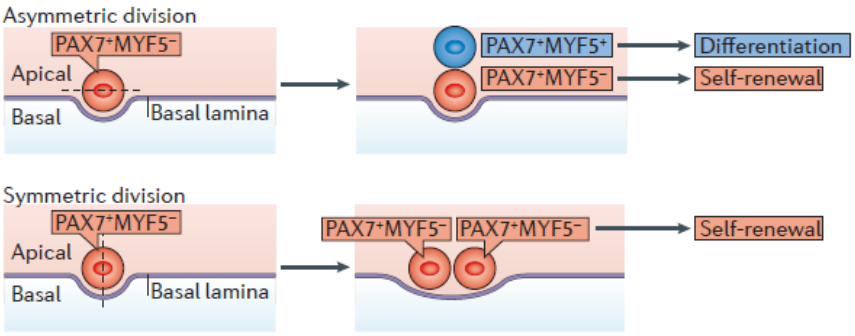

A.E. Almada and A.J. Wagers, Mol Cell Biol (2016).

Figure 2: Satellite cell model of self-renewal: apico-basal division generates one differentiating cell and one self-renewing cell by asymmetric division. Planar division generates two self-renewing cells by symmetric division.

Another proposed mechanism governing self-renewal is lineage regression. Several studies have shown that while most of the Pax7+/MyoD+ cells undergo differentiation, some of them repress MyoD expression and keep Pax7 high, acquiring the quiescence marker Nestin [22].

The type of division can depend on the distribution of cellular components to one or the other side of the cell. For example during SC division, it has been shown that the DNA strand used for replication is segregated to the self-renewing cell [23]. Also p38 α/β shows an asymmetric distribution during SC division, with the differentiating cell acquiring p38 α/β [24]. Furthermore, during asymmetric SC division, the differentiating cell expresses higher level of Notch ligand Delta1, while the self-renewing SC expresses higher level of Notch3 [19].

During stem cell division the axis of polarity is already determined during interphase. The molecular machinery composed by Par-3, Par-6 and aPKC (PAR complex) is a well conserved mechanism to establish cell polarity in different organisms. In drosophila neuroblasts, it has been shown that the PAR complex is localized to the apical side of the cell cortex, from which the self-renewing cell will generate. PAR complex is responsible for the localization

of cell fate determinants to one or the other side of the dividing cell. One of these determinants is Numb, the Notch receptor antagonist, that is localized to the basal side of the cell cortex, giving rise to the differentiated cell [25]. On the contrary, in intestinal stem cells, PAR complex localizes to the side of the cell that generates the differentiating cell [26].
In satellite cells, PAR complex localises to the side of the future differentiated cell. The localization of Pard3 (the analogous of Par3 in mammals) is regulated by Mark2 (Par1 in Drosophila), which segregates the PAR complex to the opposite side of the cell cortex.
Rudnicki's lab has shown that a protein localized to the cell membrane, called dystrophin, regulates Mark2 localization. When dystrophin is absent, Mark2 is dysregulated, and thus Pard3 polarization to the side of the cell that will differentiate, is broken. The aberrant localization of Pard3 leads to cell polarity defects, and impaired mitotic spindle orientation. As a consequence, the number of apico-basal divisions are reduced, and the number of simmetric divisions generating self-renewing cells increases [27]. Coherently, it has been shown that Pard3 knockdown causes loss of asymmetric division and impaired formation of progenitor cells [28].

1.1.3 Satellite cells in Duchenne Muscular Dystrophy

Duchenne Muscular Dystrophy (DMD) is an X-linked genetic disease caused by mutations in the dystrophin gene, a component of the dystrophin glycoprotein complex (DGC). This protein forms a link between the actin cytoskeleton of the muscle fiber and the ECM, protecting the fiber from breaking during muscle contraction. In the absence of dystrophin, muscle fibers are fragile, and muscle undergoes progressive degeneration [29]. Continuous cycles of muscle degeneration and regeneration cause chronic inflammation, which worsens the disease. Initially, skeletal muscle is able to regenerate, but eventually the regenerative ability decreases, and muscle is replaced by non-functional fibrotic tissue

[30]. Mdx mice also show defects in the satellite cell compartment, that contribute to the impaired regeneration. It has been suggested that dystrophic SCs undergo progressive exhaustion due to the continuous need for DMD muscle to regenerate [31], [32]. Moreover, one study showed that dystrophic SCs display reduced self-renewal ability, associated with attenuated Notch signaling. These evidence can further explain the reduction in stem cell pool observed in dystrophic muscle [33].
On the contrary, another study suggested that lack of dystrophin in satellite cells leads to an impairment in the asymmetric division, with an increased number of quiescent cells and a reduced number of myogenic precursors. This leads to a progressive increase in the number of quiescent satellite cells, which however, cannot participate to regeneration efficiently [27]. The mechanism by which dystrophin absence leads to increased number of quiescent cells is explained in the chapter above.
Although contrasting, all these studies agree with the fact that satellite cell defects contribute to the reduced regeneration in mdx mice. Thus, pharmacological therapies should target both the inflammation and the stem cell defects.

1.2 The immune response in skeletal muscle

1.2.1 The immune response after muscle injury

Skeletal muscle regeneration after injury is a complex phenomenon involving different cell types: satellite cells, immune cells, and other cells in the niche. The first event to take place after muscle injury is necrosis, with the disruption of the muscle fiber integrity and the release of proteins and micro-RNAs that are normally confined inside the cell. During necrosis, an increase in Calcium release causes calcium-dependent proteolysis, exacerbating the degeneration of muscle fibers [34]. Following tissue damage, released chemotactic factors orchestrate the recruitment of circulating leukocytes to the injury site. Neutrophils (CD11b+

Ly6G+) are the first inflammatory cells to infiltrate damaged tissue, peaking between 1 and 6 h after damage. Resident macrophages (CD11b+, F4/80+), attract neutrophils to the injury site by producing neutrophil chemoattractant chemokine ligands CXCL1 and CCL2. Neutrophil number remains high until 24h after injury, and then rapidly decreases. These cells phagocytose cell debris and release free radicals, proteases and pro-inflammatory cytokines. Circulating monocytes extravasate and infiltrate the site of injury within the first 24-48h [35]. Pro-inflammatory cytokines such as Tumor Necrosis Factor α (TNF-α) and interferon γ (IFN-γ), drive the differentiation of recruited monocytes into pro-inflammatory macrophages (M1), which are responsible for the perpetuation of the inflammatory response. Phagocytosis promoted by M1 macrophages and neutrophils is an important process necessary for removing dead cells and debris and preparing the tissue for the following phase of regeneration. M1 produced cytokines IL-1β, IL-6 and TNF-α are important for the induction of satellite cell activation and proliferation [36], [37]. During the regeneration phase M1 macrophages undergo a transition to M2 anti-inflammatory macrophages (CD11b+, F4/80+CD206+). M1 and M2 macrophages represent the two extremes of different subpopulations of macrophages showing intermediate phenotype. M1 and M2 macrophages can also coexist in the same area after muscle injury. M2 macrophages peak around day 4, and remain high throughout the regenerative phase. They are activated by Th2 cytokines IL-4, IL-10 and IL-13. In particular, IL-10 plays a fundamental role in the switch from M1 to M2 macrophages in injured muscle in vivo. The ablation of this cytokine inhibits this switch, exacerbating tissue inflammation and altering muscle regeneration [38].

M2 macrophages are important to sustain muscle regeneration by secreting anti-inflammatory cytokines IL-4 and IGF-1 and TGF-β. They sustain ECM matrix deposition and suppress the inflammatory response.

Myeloid cells are the most abundant immune cell types during muscle acute injury. However, CD4+ and CD8+ T cells are also present in injured muscle and play a role, although less important than myeloid cells [35]. It was found that FOXP3, the master gene of T_{reg} cells, peaks during the regenerative phase. These results suggested that T_{reg} cells may play an important role in muscle regeneration. In line with this, it was found that the suppression of this cell population leads to slowed muscle regeneration and increased inflammation. In addition T_{reg} depletion also seems to impair the normal switch from M1 to M2 macrophage phenotype [39]. It is important to state that the stages of muscle inflammation are closely associated to the stages of satellite cell activation, proliferation and differentiation. The close interaction between these type of cells will be discussed in detail in the next chapter.

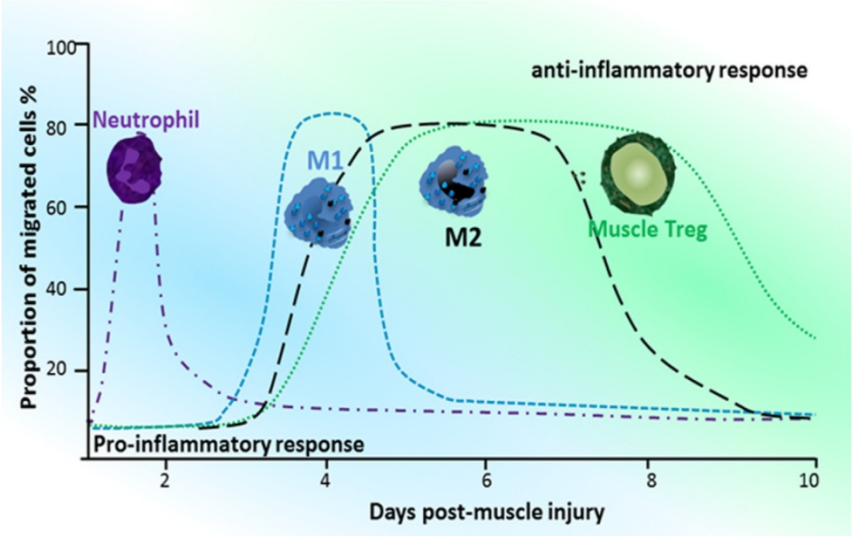

J. Saini et al. Ageing Res Rev (2016).

Figure 3: Muscle immune response after injury. Neutrophils are the first cells to peak 24h after injury, followed by M1 macrophages at day 3 after injury, and M2 macrophages at day 2-4 after injury. M2 number remains elevated for all the duration of the regenerative phase.

1.2.3 Satellite cell and immune cell crosstalk during injury

After muscle injury, neutrophils are the first cells to arrive, followed by macrophages later, which begin to express the pro-inflammatory cytokine TNF-α. The level of this cytokine peaks 24h after injury, indicating its role in the early inflammatory response and the promotion of muscle fiber damage. TNF-α induces the production of NO by myeloid cells, that is linked to fiber damage. However, TNF-α level remains elevated for the following 2 weeks after injury, suggesting a role of this cytokine also in muscle regeneration [40]. These different roles of TNF-α may depend on the cell target. If the target is macrophages, TNF-α acts by inducing their pro-inflammatory phenotype, if the target is satellite cells TNF-α stimulates their activation and proliferation. *In vivo* studies of TNF-α-null mice showed a reduced expression of MyoD and Mef-2 compared to WT, suggesting a role of this cytokine in the induction of the early differentiation phase [41]. However, *in vitro* studies showed that TNF-α acts as an inhibitor of myoblast fusion, suggesting that this cytokine acts as a negative regulator for the switch from the early to the terminal differentiation phase of SCs[42]. TNF-α can also activate NF-κB transcription factor, which induces the expression of TNF-α and IL-1 further amplifying the inflammatory response. NF-κB acts by stimulating satellite cell proliferation and inhibiting their differentiation, by promoting Cyclin D1 expression and reducing MyoD expression in satellite cells [42], [43]. Furthermore NF-κB induces IL-6 expression, a pleiotropic cytokine that amplify the proliferative anti-differentiation effects of NF-κB. However, IL-6 can also influence the late phase of differentiation, contributing to muscle formation and growth [44].
IFN-γ is another critical cytokine for the coordination of inflammation and the early regeneration stage. Neutrophils and macrophages produce IFN-γ, which peaks within the first 24h after muscle injury. However, its levels remain high up to day 5 after injury. Together with TNF-α and IL-1β, IFN-γ induces monocyte differentiation to M1 macrophages [45]. IFN-γ also binds to

myoblasts, where it activates the JAK-STAT1 pathway, inhibiting their differentiation by reducing myogenin expression and inducing the expression of genes such as CIITA. IFN-γ is thus important for the clearance of cell debris, and satellite cell proliferation [46].
Around day 3-4 after injury, an increase in IL-10 level drives the switch of macrophages from M1 to M2 phenotype, and this corresponds to the transition from the proliferation to the differentiation phase of satellite cells. As discussed in the previous chapter, the M2 macrophage population is characterized by the production of IL-10 and TGF-β, and is essential to suppress inflammation and promote muscle regeneration. Ablation of IL-10 negatively affects the macrophage switch, prolonging the inflammatory phase and severely impairing muscle regeneration. M2 macrophages secrete numerous types of ECM proteins, fibronectin and Collagen VI [47]. Besides, IL-4 and IGF-1 released by M2 macrophages are essential to induce SC differentiation. IGF-1 is also produced by myofibers, satellite cells and endothelial cells. This cytokine binds to the IGF-1 receptor and induces AKT pathway to initiate protein synthesis and inhibit protein degradation, contributing to muscle growth [48].
In conclusion, the immune system and satellite cell crosstalk during muscle injury is a finely bidirectionally regulated process. Alterations in the balance of the type and level of cytokines translates in regeneration defects.

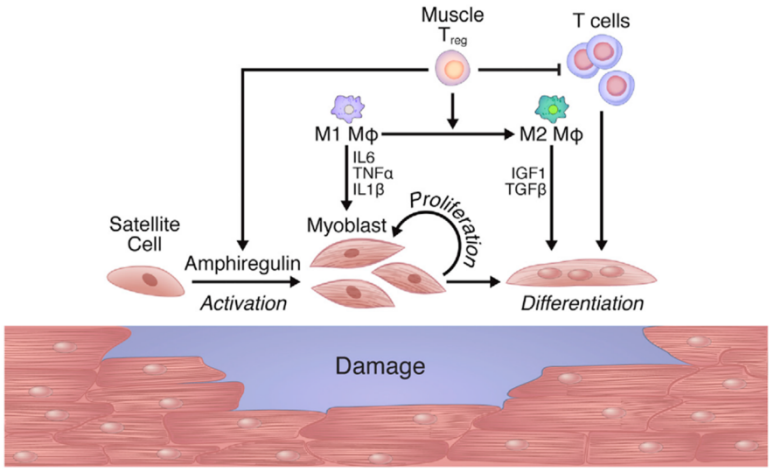

A.B. Aurora and E. N. Olson. Cell Stem Cell (2014).

Figure 4: The immune-satellite cell crosstalk. M1 macrophages secrete inflammatory cytokines with proliferative effects on myoblasts. Myotube differentiation is driven by M2 macrophage-secreted cytokines (IGF1 and TGFb). T_{regs} influences myoblast proliferation and differentiation, and are necessary for M1 to M2 macrophage polarization.

1.3 PKCθ in muscle

1.3.1 PKCθ in skeletal muscle

PKCθ is the most abundant of the PKCs expressed in skeletal muscle, where it is involved in a variety of processes regulating muscle development and homeostasis [49]. During mouse skeletal muscle development, PKCθ is expressed in foetal and post-natal but not in embryonic myoblasts *in vivo*. During skeletal myogenesis three different muscle cell precursors coexist at the same time: embryonic myoblasts, foetal myoblasts and satellite cells. However, they undergo different waves of differentiation, and the factors regulating this different response are still unknown. One of the possible mechanisms proposed is the differential response of the skeletal muscle precursors cells to TGF-β

differentiation inhibitory effect. Embryonic myoblasts usually differentiate when treated with TGF-β. However, when PKCθ is expressed ectopically in these cells, they become sensitive to the differentiation inhibitory effect of TGF-β. This results suggest that PKCθ, together with TGF-β regulate the asynchronous differentiation of the muscle precursors [50].

Another role of PKCθ in fetal myogenic development is the regulation of the fetal muscle creatin kinase (MCK) expression. MCK transcription is directly mediated by MEF2A, which is expressed already in embryonic myoblasts, but is not active. Its activation is regulated by Nuclear Factor I X (Nfix), which is selectively expressed in fetal but not in embryonic myoblasts. The proposed mechanism for MCK expression is that MEF2A binds Nfix, which recruits PKCθ that in turn activates MEF2A by phosphorylating it. A study in C2C12 supports the regulation of MEFA activity by PKCθ, showing that PKCθ interacts with calcineurin to regulate HDAC shuttling and MEF2 activation [51]. Together these results show that PKCθ is involved in the fetal skeletal muscle myogenesis.

As mentioned before, PKCθ is expressed in neonatal muscle, suggesting its potential involvement in the regulation of postnatal muscle growth. Accordingly, we observed a delay in muscle and body growth in total and muscle specific PKCθ knock out mice, during the first weeks of life. Moreover, even muscle regeneration, after induction of freeze injury was delayed in PKCθ-/- mice, compared to WT. As a further confirmation of delayed regeneration, we observed reduced expression of myogenin, but not Pax7, indicating a role of PKCθ in the regulation of myogenic differentiation. *In vitro*, we found that PKCθ is expressed in satellite cells, and reaches a peak during the initial phase of myoblast fusion. Indeed, cultured myoblast derived from PKCθ-/- mice generated smaller myotubes with less myonuclei, compared to WT. This phenotype was associated with a reduced phosphorylation/ activation of FAK (focal adhesion kinase), and a reduced expression of FAK target genes caveolin-3 and β1D-

integrin (two genes upregulated during myoblast fusion). This results suggest that PKCθ regulates the myogenic differentiation program by activating FAK [52].
In another study, it was shown that silencing PKCθ in the myoblast cell line C2C12, led to opposite results. The authors showed that $PKC\theta^{shRNA}$ C2C12 cells had increased fusion rate, with bigger myotubes and an increased rate of protein synthesis. These effects were mediated by the modulation of IRS1 and ERK1/2 phosphorylation. The discrepancy between this results and our findings may depend on the different cell system used [53].
PKCθ is also localized at the Neuro Muscular Junction (NMJ), and its expression in muscle peaks concomitantly with the NMJ maturation. Thus, PKCθ may also be involved in nerve maturation. In line with this, it was found that synapse elimination, a process normally occurring during NMJ maturation, was altered in PKCθ-/- mice [54]. However, adult PKCθ-/- mice showed normal NMJ, indicating that PKCθ may not be required for its final maturation [55].
PKCθ also regulates other pathways involved in skeletal muscle homeostasis, such as ER stress induced autophagy in C2C12 cells [56]. Furthermore, PKCθ controls the sarcolemma electrical activity by regulating the CIC-1 chloride channel [57].

Stage	Experimental observations	Experimental model	Suggested role
Muscle development	PKCθ is expressed in fetal muscle and co-operates with *Nfix* and MEF2A in the activation of fetal-specific muscle genes	*In vivo/in vitro*	Control of secondary myogenesis *in vivo*
Myogenesis	PKCθ regulates HDACs nucleus/cytoplasm shuttling and co-operates with CN in MEF2-dependent muscle-gene expression	*In vitro*	Control of MEF2 activity in regulating muscle-specific gene expression
Myogenesis	PKCθ expression peaks in the early stages of differentiation in SCs and regulates the expression of pro-fusion genes required for myoblast fusion	*In vivo/in vitro*	Control of myofibre growth and regeneration
Nerve–muscle interaction	PKCθ expression is nerve regulated, it localizes at the NMJs and its ablation prevents synapse elimination and maturation	*In vivo/in vitro*	Control of neuromuscular interaction
Muscle maintenance	PKCθ mediates ER-stress-induced autophagy and its ablation prevents starvation- and immobilization-induced muscle atrophy	*In vitro/in vivo*	Control of muscle adaptation to environmental cue and remodelling
Muscle maintenance	PKCθ ablation results in increase of ClC-1 channel activity, reduced muscle excitability and alteration of muscle phenotype	*In vivo*	Control of myofibres activity and phenotype
Muscle diseases	PKCθ ablation ameliorates muscular dystrophy	*In vivo*	Control of inflammatory response in degenerating muscle

V. Marrocco et al. Biochem Soc Trans (2014).

Figure 5: Summary of the multiple roles of PKCθ in skeletal muscle homeostasis, maintenance and disease.

1.3.2 PKCθ and the immune system

Protein kinase C Theta (PKCθ) is a serine and threonine kinase belonging to the family of PKCs, which is composed of 3 subclasses: classic PKCs (cPKCs), novel PKCs (nPKCs) and atypical PKCs (aPKCs). All PKCs are composed of a C-terminal catalytic domain with a lipid binding domain, a N-terminal regulatory domain, for the Ca^{++}- dependent binding to membrane phospholipids, and a flexible domain in between, called V3 domain. The 3 subclasses of PKCs differ in the regulatory domain structure and the cofactors needed for activation. The cPKCs

require for their activation both binding to DAG and Ca^{++}. The nPKCs only require DAG but not Ca^{++} for the activation, while the aPKC do not require DAG nor Ca^{++} [58]. PKCθ belongs to the class of the novel PKCs, and its structure has been solved by Xu et al. These researchers showed that there are two main conformations for PKCθ: open/active and closed/ inactive. The switch from the closed state to the open state involves the biding to DAG, and the phosphorylation of Thr-538, which is fundamental for kinase activation [59]. PKCθ is mainly expressed in hematopoietic cells, in particular in T cells, but also in mast cells, natural killer cells and platelets [60], [61], [62]. PKCθ is also the most abundant PKC expressed in skeletal muscle [63], where it mediates insulin resistance associated with type 2 diabetes [64]. PKCθ best characterized role however, is that in T cells, where it regulates cell activation and proliferation. When a T cell recognizes an antigen presenting cell, a tight junction called immunological synapse forms at the site where the T cell receptor (TCR) binds to the peptide-MHC complex. PKCθ is selectively recruited to the immunological synapse in conventional and effector T cells, where it directs signal transduction cascade. PKCθ activation regulates the expression of NF-kB, AP-1, and NFAT, three genes fundamental for T cell function. In addition, PKCθ can regulate gene expression by physically associating with chromatin and inducing genes associated with the immune response [65].
PKCθ knock out mice (PKCθ-/-) are healthy and live normally, and show a normal development of T cells in the thymus [66]. However, PKCθ-/- mice show a severely impaired Th2 response. Following TCR binding to MHC, PKCθ-/- mice display a reduction in the production of IL-2, with a consequent defective proliferation of T cell, and impaired NF-kB and AP-1 activation [67]. Despite these findings, Berg-Brown et al. showed that PKCθ-/- mice could mount an immune response against vesicular stomatitis virus (VSV) infection. This, together with other studies led to the finding that PKCθ-/- is dispensable for the immune response against viruses and bacteria. This apparently contradictive

response can be explained by the fact that other mechanisms such as innate immune responses can compensate for the absence of PKCθ. Therefore, the innate immune response can overcome the need for a $CD8^+$ T cell response [68].

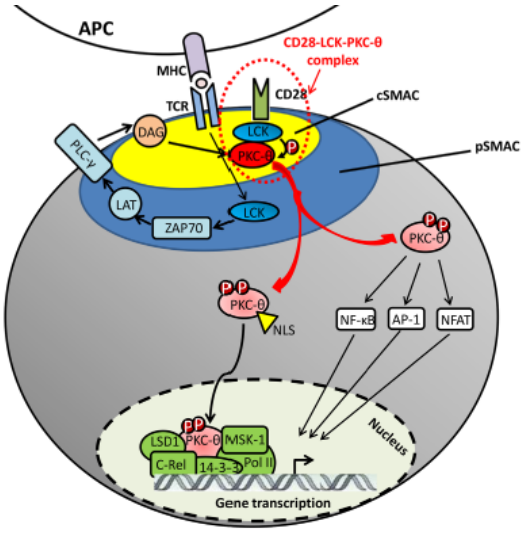

Brezar et al. Front. In Immunol. (2015)

Figure 6: PKCθ localized to the immunological synapse in T_{eff} cells, where it regulates their activation and proliferation by inducing NF-kB, AP-1, and NFAT activation.

Also T_{reg} cells express PKCθ. These cells are important regulators of $CD4^+$, $CD8^+$, NK, and B cell responses. PKCθ-/- mice showed impaired T_{reg} development in the thymus, with a consequent reduced number of T_{reg} in the periphery, although not completely suppressed [69][70]. However, T_{reg} isolated from PKCθ-/- mice showed a normal suppressive activity *in vitro*. Although some studies identified PKCθ as a necessary enzyme for T_{reg} differentiation, some other studies found that PKCθ inhibition actually enhances T_{reg} cell suppressive activity [71]. These discrepancies have yet to be elucidated. However, what emerges from these findings is that T_{reg} activity is not significantly

compromised following PKCθ inhibition. This, together with the finding that PKCθ is not necessary for T_{eff} cell response against viruses and bacteria, makes PKCθ a promising target for the treatment of diseases requiring immune modulation.

1.3.3 Targeting PKCθ in Duchenne Muscular Dystrophy

As discussed above, PKCθ plays an essential role in the immune response. Lack of PKCθ inhibits T_{eff} cell function without significantly compromising T_{reg} suppressive activity. For this reason PKCθ inhibition has been proposed for the treatment of immune diseases, such as autoimmune diseases, graft versus host disease, Th2 and Th17 mediated inflammatory diseases [58]. In our laboratory we tested the therapeutic effect of PKCθ inhibition for the tratment of a chronic muscle inflammation in Duchenne Muscular Dystrophy (DMD). The only available therapy for DMD is glucocorticoid treatment, general immunosuppressors which initially slow down the disease progression, but are associated with many adverse effects. Works from our lab in the mdx mouse, the animal model for DMD, showed that $CD3^+$ T cells (CD4+ and CD8+) are among the first cells to infiltrate dystrophic muscle, prior to the onset of necrosis. These findings identified T cells as one of the main cell populations orchestrating the early acute inflammatory response in mdx mice. Pharmacological inhibition of PKCθ with C20, a very potent and selective inhibitor of PKCθ, led to a significant reduction in T cells, but also neutrophils, macrophages and eosinophils recruited to dystrophic muscle. Reduced inflammation was associated with reduced muscle degeneration, reduced collagen deposition and improved muscle performance [72], [73]. Similar results were obtained with the PKCθ-/- mouse model [74].

Interestingly, in our mdx PKCθ-/- mouse model, although muscle damage was reduced, we found that muscle regeneration was increased (Figure 7A). The increased muscle regeneration was

associated with an increase in satellite cell number up to late stages of the disease, such as 12 months of age (Figure 7B). Furthermore, we found an increase in Notch expression in satellite cells isolated from mdx PKCθ-/-, suggesting that self-renewal may be facilitated in absence of PKCθ (Figure 7C), (Fiore P. et al. Int J Mol Sci. *Accepted*). Together these results suggest that PKCθ inhibition in mdx mice is able to ameliorate the disease phenotype by reducing inflammation and by possibly improving satellite cell function.

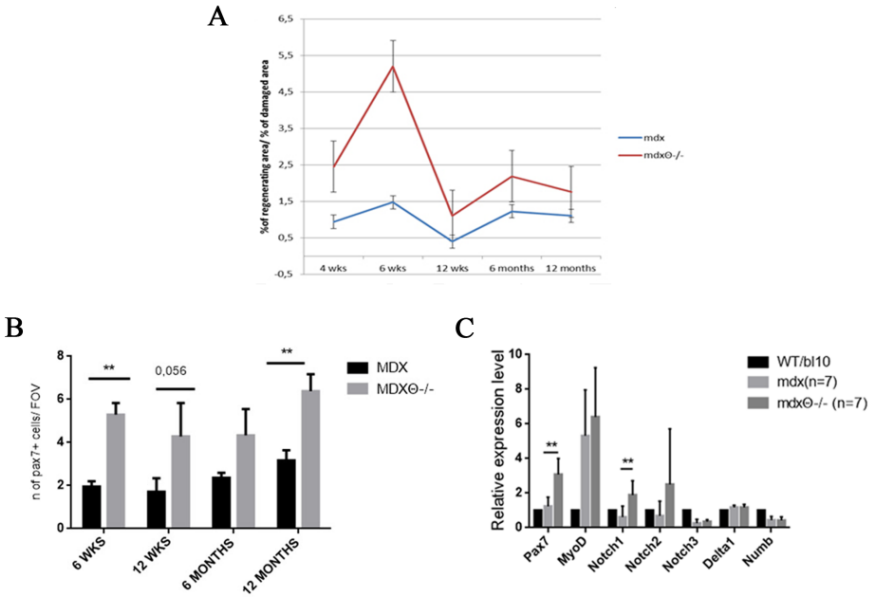

Fiore P. et al. Int J Mol Sci (2020)

Figure 7: A: The ratio between muscle regeneration and degeneration is always higher in mdx PKCθ-/- mice compared to mdx. B: SC number is increased in mdx PKCθ-/- mice up to 12 months of age. C: SCs isolated from mdx PKCθ-/- mice at 6 wks of age express higher level of Notch1 compared to mdx mice.

2. AIMS OF THE THESIS

Our preliminary results in mdx PKCθ-/- mice suggest that lack of PKCθ improves regeneration and influences satellite cell function. Indeed, we observed an improved regenerative ability in mdx PKCθ-/- mice compared to control, even at later stages of the disease, which should be due predominantly to changes in the inflammatory response. However, there might be also a direct effect on SCs. Indeed, mdx PKCθ-/- mice show an increase in the number of satellite cells, which express higher level of Notch compared to mdx mice, indicating that self-renewal may be facilitated in the absence of PKCθ. Thus, we speculated that PKCθ may control satellite cell behavior via direct and/or indirect pathways (such as immune cell crosstalk).

2.1 To investigate the direct role of PKCθ in satellite cell function

To understand whether PKCθ influences SC function directly, we studied PKCθ expression kinetics and its localization in satellite cells. We then analyzed the effect of PKCθ absence/ inhibition on self-renewal *in vitro*, by studying satellite cell symmetric/asymmetric division and Pax7/MyoD expression on single myofibers. To understand whether PKCθ influences satellite cell self-renewal *in vivo*, we analyzed the effect of PKCθ absence/inhibition on satellite cell number in steady state and after muscle injury.

2.2 To investigate the indirect pathways by which PKCθ influences the satellite cell compartment

It is known that satellite cell behaviour is strongly influenced by the inflammatory environment [75]. PKCθ regulates T cell activation and proliferation, and in the context of chronic muscle inflammation is important for T cell recruitment. On the other hand, its role in neutrophil and macrophage responses, which are

known to affect SC ability to regenerate muscle, is less clear [58]. To understand whether PKCθ also influences myeloid cell infiltration we used a model of acute muscle injury, where neutrophils and monocytes but not T cells predominate during the first week following injury. Following intra-muscular injection of cardiotoxin (CTX) in WT and PKCθ-/- mice we analyzed the quality and quantity of the inflammatory infiltrate by flow-cytometry at 3 and 10 days after injury, during the inflammatory and the regenerative phase respectively. We also analyzed the production of inflammatory cytokines by Real Time PCR. These experiments helped to clarify whether PKCθ regulates the recruitment and activity of innate immune cells known to influence satellite cell ability to regenerate muscle.

3. RESULTS

3.1 PKCθ is expressed in satellite cells

3.1.1 PKCθ is expressed in freshly isolated and differentiating satellite cells, and it is downregulated in proliferating cells

Satellite cells can exist in a quiescent state in physiological conditions, or as activated/committed progenitors during muscle regeneration. To elucidate the functional role of PKCθ in satellite cells, we first analyzed the kinetics of PKCθ expression by real time PCR (rtPCR) during myogenic differentiation. Satellite cells were isolated by magnetic bead labeling from WT hindlimb muscles, before or after CTX injury.
It is known that after isolation satellite cells become activated. Indeed, the isolation procedure leads to their dissociation from the fiber, causing profound transcriptomic and epigenetic modifications, compared to quiescent cells [76].
To investigate whether PKCθ is expressed in early activated cells, PKCθ was analyzed in freshly isolated satellite cells from uninjured muscle.
PKCθ expression was also analyzed in satellite cells isolated from regenerating muscle at 3, 5 and 7 days after CTX injury. Interestingly, rtPCR analysis showed that PKCθ expression is high in early activated cells and drastically decreases in cells isolated from 3 day-injured muscle, corresponding to the proliferation phase, *in vivo*. PKCθ expression then increases in cells isolated from 5 and 7 day-injured muscle, corresponding to the regeneration phase (Figure 8).
To confirm the differential expression observed by rtPCR, we examined PKCθ expression by western blot analysis in cultured myoblasts. Satellite cells were isolated by magnetic bead labeling and cultured in growth medium (GM) for 72h, and subsequently in differentiation medium (DM) for 24h, to analyze PKCθ expression

in proliferating and differentiating cells respectively. Another subset of satellite cells was collected for analysis immediately after isolation to analyze PKCθ expression in activated cells. Western Blot analysis showed that PKCθ is already expressed in activated cells, its expression declines in proliferating cells and increases again in differentiating cells (Figure 9A and B). The analysis of the phosphorylated/active form instead, revealed that the ratio between p-PKCθ and PKCθ was maximal at 72h in GM, during the proliferative phase (Figure 9A and C).

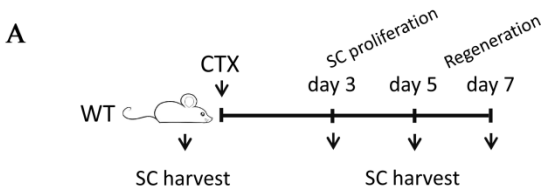

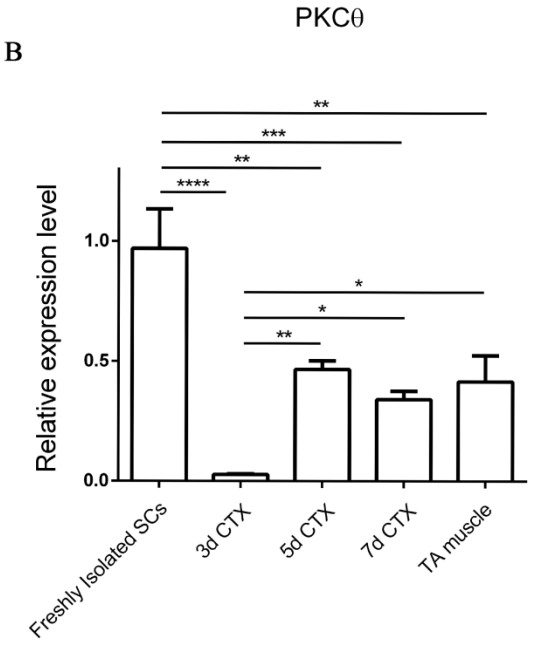

Figure 8: A: experimental design. B: rtPCR showing PKCθ expression in freshly isolated SCs (n = 9 mice) and SCs isolated from 3, 5 and 7 day-injured WT muscles (n ≥ 4 mice per group). Total RNA extract from WT tibialis muscle was used as positive control. GAPDH was used for normalization. Error bars represent mean ± sem, *p < 0.05, **p < 0.01, ***p < 0.001, ****p < 0.0001 calculated by One-way Anova with adjustment for multiple comparison test.

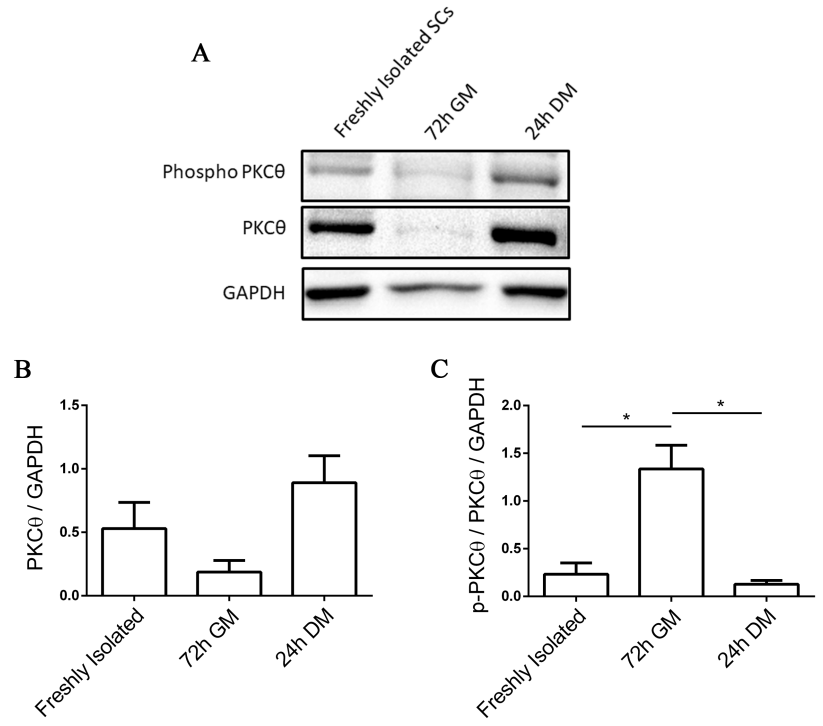

Figure 9: A: WB analysis showing PKCθ expression in activated SCs (freshly isolated), proliferating SCs (72h GM), differentiated myotubes (24h DM) (n= 3 individual experiments). B: Densitometry of WB analysis showing PKCθ expression normalized on GAPDH protein. C: Densitometry of WB analysis showing p-PKCθ/ PKCθ ratio, normalized on GAPDH protein. Error bars represent mean ± sem, *p < 0.05 calculated by One-way Anova with adjustment for multiple comparison test.

3.1.2 Phospho-PKCθ is localized to the chromosomes, centrosomes and midbody of dividing satellite cells

PKCθ shows two conformational states: one closed/inactive and one open/active [58]. The transition to the active state requires binding to the DAG and T538 phosphorylation. To understand the specific role of PKCθ in satellite cells, we assessed its activation and localization in cultured satellite cells.
To this aim we isolated satellite cells from WT mice and cultured them for 72h in GM. After 72h in culture we performed immunofluorescence analysis of phospho-PKCθ and α-Tubulin, to visualize the mitotic spindle.
At 24h of culture in GM a diffused phospho-PKCθ immunostaining was visible on satellite cell membrane (Figure 10A). At 72h in culture in growth medium, satellite cells are proliferating. At this stage it was possible to distinguish the different phases of mitosis thanks to the nuclear shape.
The results showed a diffused membrane localization of phospho-PKCθ during interphase. During prophase phospho-PKCθ moves to the nucleus, where chromatin is condensating. During metaphase phospho-PKCθ immunostaining is detectable close to the centrosomes, and partially to the mitotic spindle. In telophase phospho-PKCθ is visible at the spindle midzone, and during cytokinesis it moves to the intercellular bridge of the midbody (Figure 10B).
These results suggest that PKCθ could be involved in the regulation of satellite cell division processes.

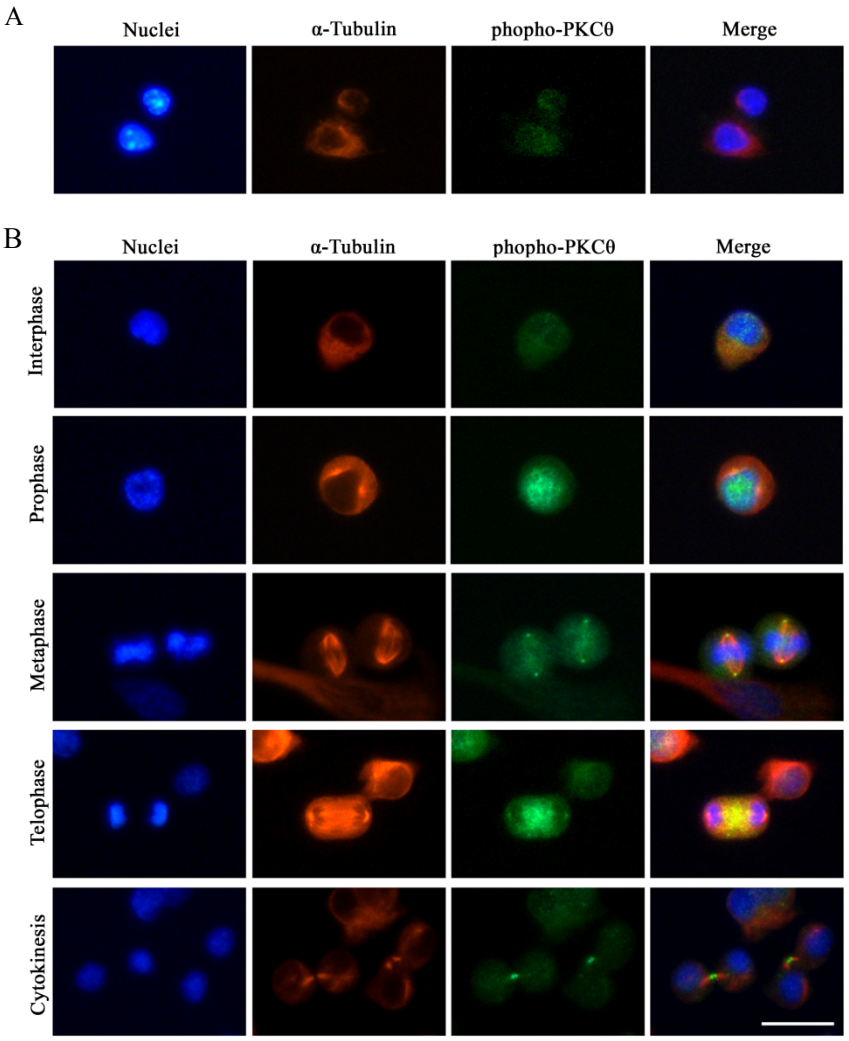

Figure 10: Representative immunofluorescence images of satellite cells after 24h (A) and 72h in culture (B), stained for α-Tubulin (red) and phospho-PKCθ (green). Nuclei were counterstained with Hoechst. Scale bar 20 μm.

3.1.3 Satellite cell proliferation is not influenced by PKCθ

The localization of phospho-PKCθ to the chromatin, centrosomes and midbody of dividing satellite cells, suggested that PKCθ could be involved in the regulation of satellite cell division.
To understand whether satellite cell proliferation is affected by PKCθ, we analyzed proliferation both *in vitro* and *in vivo*. For the *in vitro* analysis, SCs were isolated from WT and PKCθ-/- muscles and cultured in growth medium in the presence of CellTrace CFSE Cell Proliferation Kit. CFSE is used to detect different generations of dividing cells by analyzing die dilution by flow-cytometry. After 72h of culture in GM with CFSE, satellite cell proliferation was analyzed. As shown, no difference was observed in CFSE fluorescence between WT and PKCθ-/- cells (Figure 11B), suggesting that the cells underwent similar rounds of cycling. Cell proliferation was also analyzed in regenerating gastrocnemius (GA) muscles *in vivo*, 3 and 7 days after CTX injury during the peak of SC proliferation and the initial phase of regeneration respectively, by immunofluorescence staining for Ki67 and Pax7. The number of cells double positive for Pax7 and Ki67 were counted, and the results were normalized to the total number of Pax7+ cells. As shown in Figure 11C, the percentage of proliferating SCs (Pax7+/Ki67+) was similar between WT and PKCθ-/- mice.
These results indicate that satellite cell proliferation is not influenced by PKCθ, neither *in vitro* nor *in vivo*.

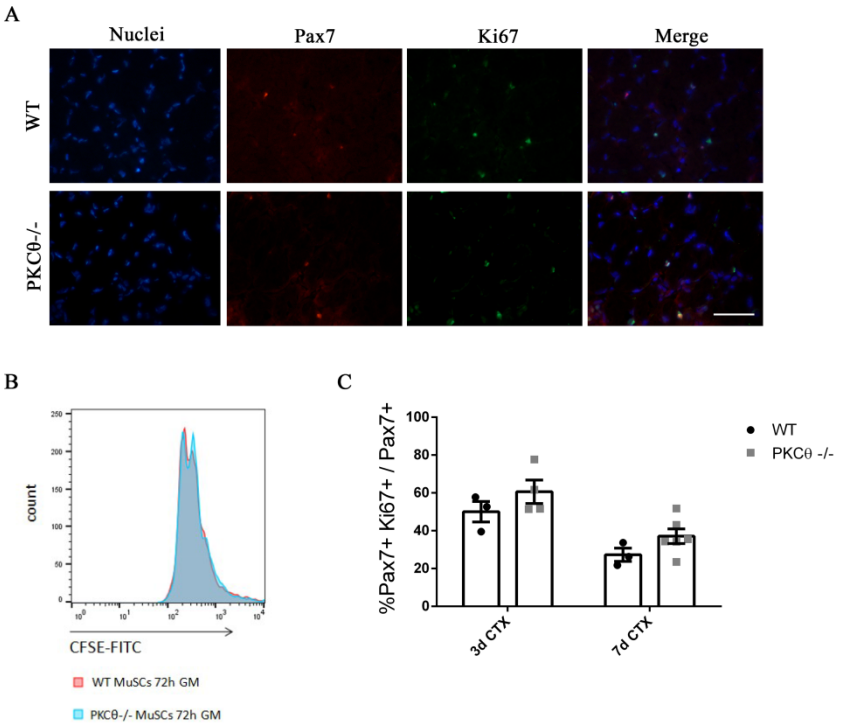

Figure 11: A: Representative immunofluorescence images of WT and PKCθ-/- GA muscles, stained for Pax7 and Ki67, 3 days after the induction of CTX injury, scale bar: 100µm. B: Flow-cytometry analysis of CFSE stained WT and PKCθ-/- SCs, cultured for 72h in GM. C: Quantification of proliferating SCs, counted by immunofluorescence for Pax7 and Ki67 on WT and PKCθ-/- GA muscle sections, 3 and 7 days after CTX injury.

3.2 Lack of PKCθ increases satellite cell self-renewal *in vitro*

3.2.1 Lack of PKCθ increases the number of 'self renewing' SCs by promoting symmetric division

In stem cells, centrosomes and mitotic spindle orientation determine whether the outcome of a cell division is symmetric or asymmetric. In T cells, PKCθ promotes MTOC reorientation and cell polarization in the direction of the antigen presenting cell. This process may also promote asymmetric division, that is important for the acquisition of T cell memory [77]. The localization of phospho-PKCθ at the centrosomes and mitotic spindle of dividing satellite cells, led us to hypothesize that this protein may be involved in the regulation of symmetric/asymmetric division.
To investigate this possibility we isolated single myofibers from WT and PKCθ-/- EDL muscles, and cultured them for 48h, the time necessary for the first cell division to occur. In this system satellite cells are not dissociated from their fiber, allowing to keep them in a niche-like environment. When myofibers are cultured satellite cells become activated, upregulate MyoD and enter cell cycle. The cells that undergo self-renewal will be positive for Pax7 and negative for MyoD, whilst satellite cells committed to differentiation will express MyoD. After 48h in culture cell doublets were visible, and symmetric/asymmetric division was studied by immunofluorescence staining for Pax7 and MyoD. We observed a significant increase in the number of symmetric satellite cell division in myofibers isolated from PKCθ-/- mice, compared to WT (Figure 12B). Within the symmetric division events, the number of 'self-renewing' Pax7+/MyoD- cell doublets was significantly higher in myofibers from PKCθ-/- mice compared to WT (Figure 12C).
Consistent with this result, also the number of total Pax7+/ MyoD- single cells was higher in PKCθ-/- myofibers, compared to the ones isolated from WT mice (Figure 12D).

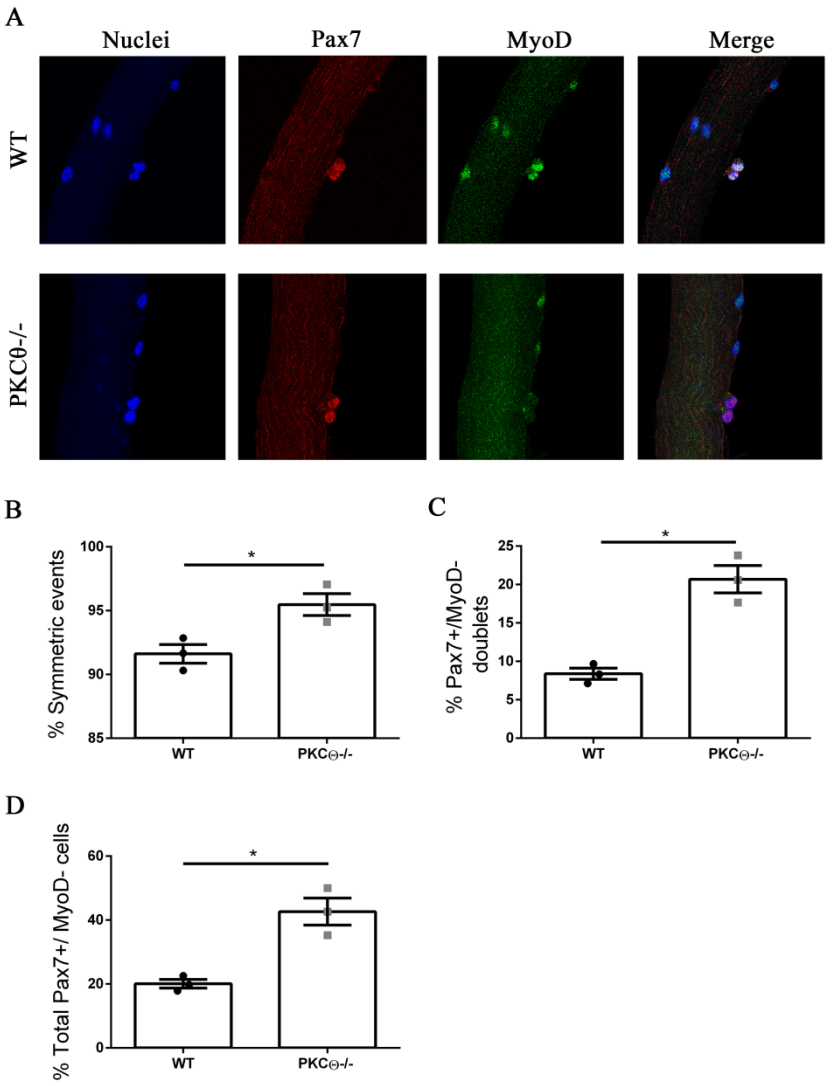

Figure 12: A: Representative pictures of single myofibers isolated from EDL muscles of WT and PKCθ-/- mice, after 48h in culture. Myofibers were stained for Pax7 (red) and MyoD (green) after 48h of culturing, nuclei were counterstained with Topro3. B: Quantification of symmetric division events. C:

Quantification of Pax7+/MyoD- cell doublets, and D: quantification of total Pax7+/MyoD- cells in WT and PKCθ -/- single myofibers. (WT, n = 3 mice, PKCθ-/-, n = 3 mice, n > 20 myofibers analyzed per mouse). Error bars represent mean ± sem, *$p < 0.05$ calculated by Student's t-test.

To understand whether the increased number of 'self-renewing' satellite cells is maintained after further divisions, we cultured single myofibers from WT and PKCθ-/- mice for 72h. After this time in culture satellite cells have proliferated, and cell clusters are visible on the myofiber surface. Pax7 and MyoD immunofluorescence revealed that the number of 'self-renewing' (Pax7+/MyoD-) cells was significantly higher in PKCθ-/- fibers compared to the WT ones. The fraction of Pax7+/MyoD+, and Pax7-/MyoD+ satellite cells, was reduced in PKCθ-/- myofibers instead (Figure 13B). The number of satellite cells per cluster was similar between the two genotypes, suggesting again that PKCθ does not affect satellite cell proliferation (Figure 13C).
Together, these results suggest that PKCθ absence increase satellite cell self-renewal *in vitro* by promoting symmetric cell division.

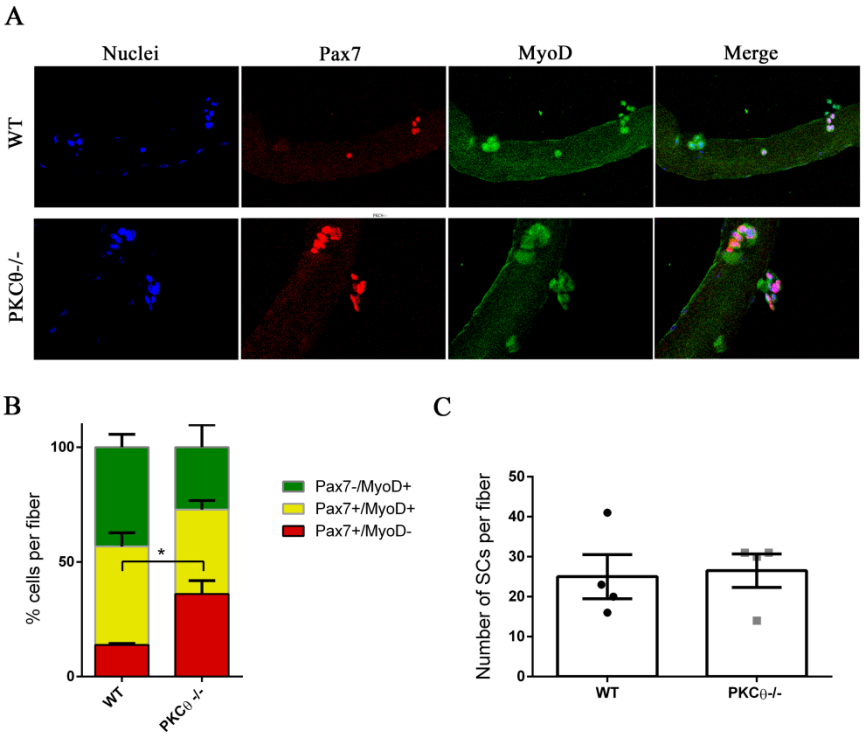

Figure 13: A: Representative pictures of single myofibers isolated from EDL muscles of WT and PKCθ -/- mice. Myofibers were stained for Pax7 and MyoD after 72h of culturing, nuclei were counterstained with Topro3. B: Quantification of SCs per fiber, single or double positive for Pax7 and/or MyoD. C: number of SCs per fiber in WT and PKCθ -/- single myofibers. (WT, n = 4 mice, PKCθ-/-, n = 4 mice, n = 100 cells analyzed per group). Error bars represent mean ± sem, *$p < 0.05$ calculated by Student's t-test.

3.2.2 C20 treatment in cultured primary myoblasts increases the fraction of reserve cells

As described above, lack of PKCθ leads to increased satellite cell self-renewal *in vitro*. We next analyzed whether pharmacological inhibition of PKCθ with C20 might lead to similar results as

genetic ablation of PKCθ in cultured satellite cells. To answer this question, we cultured primary satellite cells from hind limb muscles of WT and PKCθ-/- mice, in presence of a PKCθ inhibitor, the C20. To analyze the effects of C20 throughout the different phases of myogenic progression, the cells were cultured for 4 days in growth medium (GM), and for 2 days in differentiation medium (DM). C20 was used at different concentration: 0.5 μM, 1 μM and 2 μM. These concentrations were already shown not to be toxic for *in vitro* and *in vivo* treatment [78], [72]. Control cultures were treated with DMSO at the same concentration used for C20 dilution. To analyze any possible indirect effect of C20, we treated PKCθ-/- satellite cells with C20, at the maximum concentration used for the experiment (2 μM).
Treatment with C20 significantly increased the fraction of Pax7+/MyoD- reserve cells in a dose dependent manner (Figure 14A and B). In parallel, the fraction of cells committed to differentiation Pax7-/MyoD+ was reduced (Figure 14C). Fusion index was also reduced after treatment with C20, but the reduction was significant only at the highest dose of C20 used (Figure 14D). Similar results were obtained analyzing the phenotype of the PKCθ-/- cultured cells. Treatment of PKCθ-/- cells with C20, did not show any difference compared to the non-treated PKCθ-/- cells, instead (not shown). These results together suggest that pharmacological inhibition of PKCθ with C20 increases the fraction of 'self-renewing' satellite cells in culture.

A

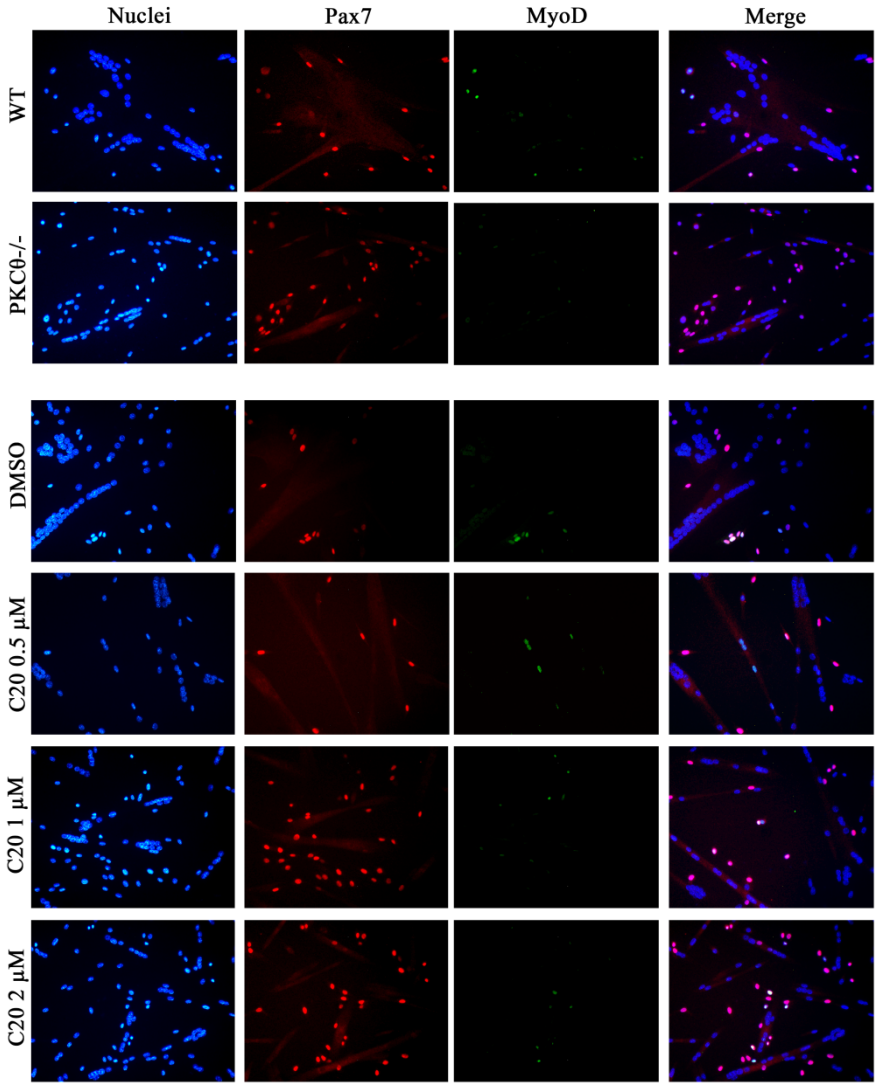

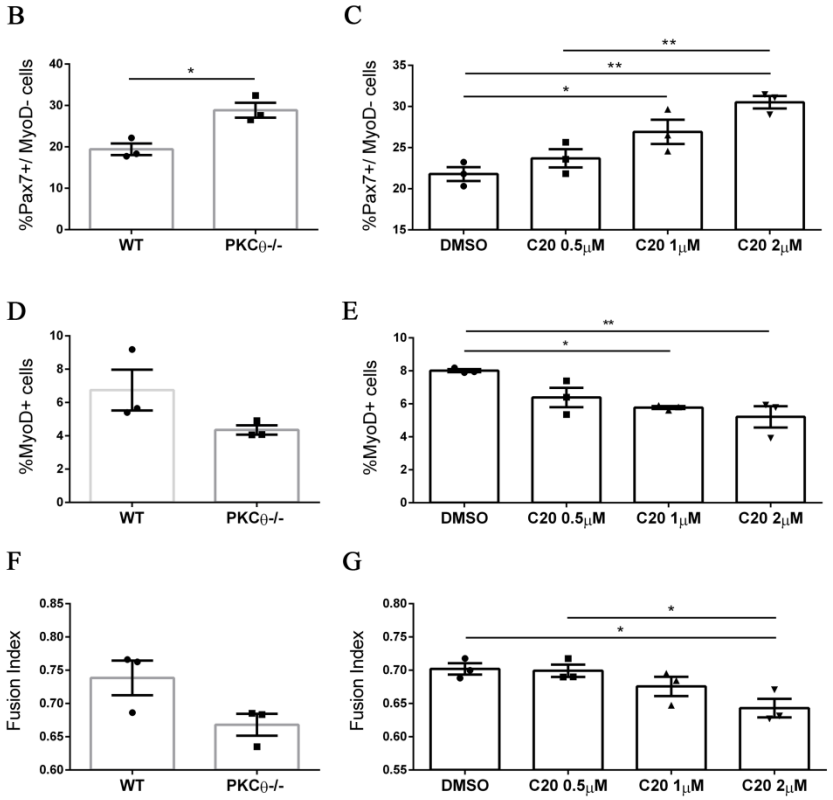

Figure 14: A: Representative pictures of PKCθ-/- and WT SCs, cultured or not with C20 at the concentration of 0.5, 1 and 2 μM (or DMSO as control). The cells were stained for Pax7 (red) and MyoD (green) after culturing for 4 days in GM and 2 days in DM. Nuclei were counterstained with Hoechst. B: percent of Pax7+/MyoD- SCs in WT and PKCθ-/- cultures, or in WT cultures treated with C20 (C). D: Percent of total MyoD+ SCs in WT and PKCθ-/- cultures, or in WT cultures treated with C20 (E). F: Fusion index of WT and PKCθ-/- myotubes, or WT myotubes treated with C20 (G) after culturing for 4 days in GM and 2 days in DM. (n = 3 replicate dishes per group). Error bars represent mean ± sem, *p < 0.05, **p < 0.01 calculated by One-way Anova with adjustment for multiple comparison test.

3.3 Genetic and pharmacological ablation of PKCθ expands satellite cell reservoir after acute injury

3.3.1 The pool of quiescent satellite cells is amplified in PKCθ-/- mice 28 days after injury

The immunofluorescence analysis performed on WT and PKCθ-/- myofibers *in vitro*, suggested that PKCθ is implicated in the regulation of satellite cell self-renewal. To understand whether PKCθ absence leads to similar results *in vivo* as well, we analyzed the number of satellite cells in WT and PKCθ-/- mice, before and after the induction of Cardiotoxin (CTX) injury.
To study satellite cell self-renewal *in vivo* we analyzed the number of satellite cells in WT and PKCθ-/- mice 7 and 28 days after injury, when the muscle is regenerating or is completely regenerated respectively. Contralateral uninjured muscle was used as control.
Immunofluorescence analysis of Pax7+ cells revealed that the number of satellite cells per mm^2 and the number of satellite cells per fiber was similar in PKCθ-/- and WT gastrocnemius (GA) muscles in uninjured conditions. 7 days after injury, the number of Pax7+ cells was increased in both WT and PKCθ-/- mice, as a result of cell proliferation. However, the number of Pax7+ cells in PKCθ-/- mice was significantly higher compared to WT mice (Figure 15). 28 days after CTX injury when muscle is completely regenerated and satellite cells have returned to quiescence, the number of Pax7+ cells is significantly higher in PKCθ-/- muscle compared to the injured WT, with an increment of 64.4% (Figure 16B and C). To confirm that at this stage all of the satellite cells have gone back to quiescence, we analyzed their cycling status by immunofluorescence staining for Pax7 and Ki67. The result showed that more than 99% of the Pax7+ cells were negative for Ki67 in both WT and PKCθ-/- mice, indicating that they are not proliferating cells (Figure 16F). Moreover, all the cells analyzed 28

days after CTX were located in the final position of quiescent cells, beneath the basal lamina and the sarcolemma of muscle fibers (Figure 16A).
This observation demonstrates that satellite cells returned to homeostatic conditions 28 days after CTX in WT and PKCθ-/- mice, and the pool of quiescent satellite cells is amplified in the absence of PKCθ-/-.
To compare the regenerative ability of WT and PKCθ-/- mice, we analyzed myofiber CSA 28 days after injury (Figure 16 D and E), and we observed that the mean myofiber CSA, and the distribution of myofiber CSAs were similar in WT and PKCθ-/- mice. These results suggest that lack of PKCθ increases satellite cell self-renewal without affecting muscle regenerative ability after injury.

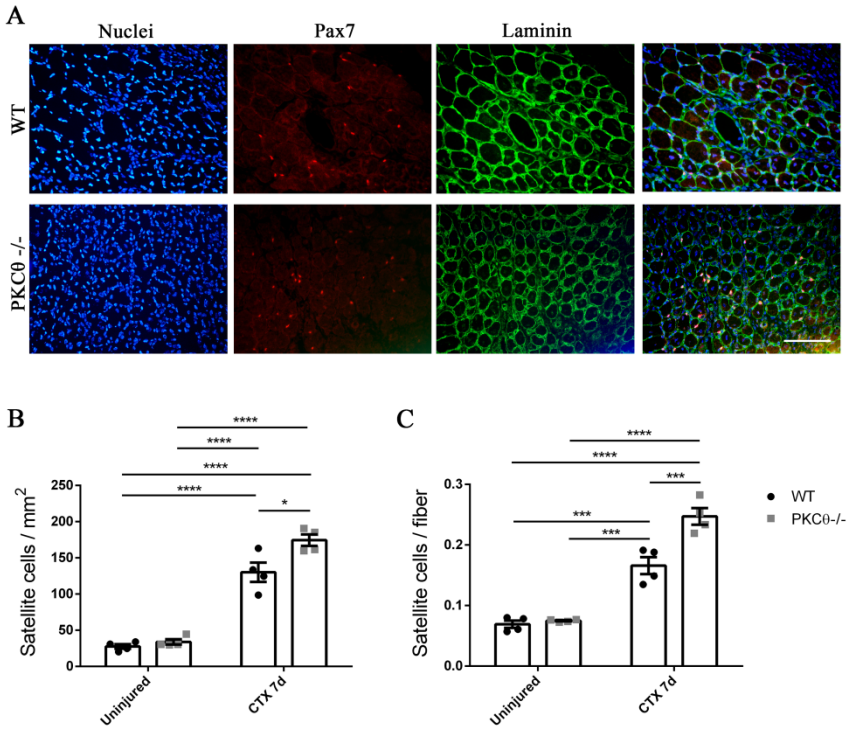

Figure 15: A: representative immunofluorescence pictures of WT and PKCθ-/- GA sections, 7 days after CTX injury. Sections were stained for Pax7 (red) and Laminin (green). Nuclei were counterstained with Hoechst. Scale bar: 100µm. B: quantification of the number of SCs per mm^2 and C: number of SCs per fiber in uninjured and 7 day-injured GA muscle, in WT and PKCθ-/- mice (WT, n = 4 mice, PKCθ-/-, n = 4 mice). Error bars represent mean ± sem, *p < 0.05, **p < 0.01, ***p < 0.001, **** p < 0.0001 calculated by Two-way Anova with adjustment for multiple comparison test.

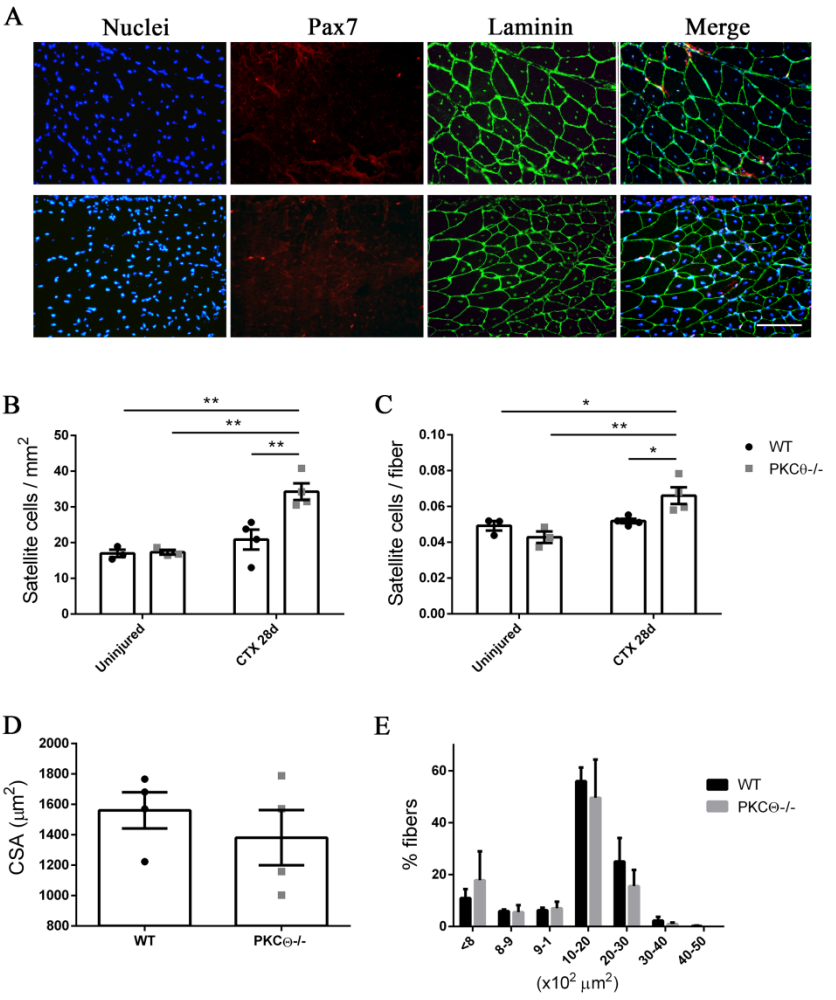

F

% Ki67- Pax7+/ Pax7+ SCs	
WT	**PKCθ-/-**
99.88 ± 0.116	99.96 ± 0.04

Figure 16: A: representative immunofluorescence pictures of WT and PKCθ-/- GA sections, 28 days after CTX injury. Sections were stained for Pax7 (red) and Laminin (green). Nuclei were counterstained with Hoechst. Scale bar: 100μm. B: quantification of the number of SCs per mm^2 and C: number of SCs per fiber in uninjured and 28 day-injured GA muscle, in WT and PKCθ-/- mice. D: mean CSA and E: CSA distribution of muscle fibers in WT and PKCθ-/- GA sections, 28 days after injury. F: quantification of non proliferating SCs 28 days after CTX injury, in WT and PKCθ-/- GA, analyzed by immunofluorescence staining for Pax7 and Ki67. (WT, n = 4 mice, PKCθ-/-, n = 4 mice). Error bars represent mean ± sem, *$p < 0.05$, **$p < 0.01$, ***$p < 0.001$, **** $p < 0.0001$ calculated by Two-way Anova with adjustment for multiple comparison test.

3.3.2 Pharmacological inhibition of PKCθ expands the pool of quiescent satellite cells after injury

As we already demonstrated, lack of PKCθ leads to expansion of the satellite cell pool after induction of CTX injury.
To investigate whether pharmacological inhibition of PKCθ leads to similar results, we treated WT mice with the pharmacological inhibitor of PKCθ (C20), and we analyzed satellite cell number before and after CTX injury. C20 is a highly potent and selective inhibitor of PKCθ, which has been already used in our lab to test its ability to counteract the dystrophic phenotype in a mouse model of Duchenne Muscular Dystrophy, the mdx mouse [72], [73]. In those studies we showed that C20 treatment administered to mdx mice for 2 weeks , is able to successfully inhibit PKCθ, without causing any major collateral effect.
Thus, we injured GA muscles of WT mice by CTX injection, and we treated the mice with daily intra peritoneal injections of C20, at a dose of 5 mg/Kg (previously established to be effective in vivo, [78]). Control mice were treated with Vehicle (DMSO) at the same concentration used to dissolve C20. Treatment was started one day prior to the CTX injection, and was continued for 10 days following injury, during the phase of satellite cell activation, proliferation and differentiation (Figure 17A). Satellite cell number was then analyzed by Pax7 immunofluorescence 28 days after injury, in the injured GA and in the contralateral uninjured GA.

The results showed that the number of Pax7+ cells per mm^2, and the number of Pax7+ cells per fiber was similar in uninjured GA in C20 and Vehicle treated mice. However, the number of satellite cells that returned to quiescence 28 days after injury, was significantly higher in mice treated with C20, compared to Vehicle treated ones, with an increment of 50% (Figure 17C and D). The analysis of the mean CSA and the CSA distribution of myofibers showed no significant differences between C20 and Vehicle treated mice, indicating that C20 treatment does not affect muscle regenerative ability (Figure 17E and F). These results suggest that C20 can be used *in vivo* to target satellite cell self-renewal.

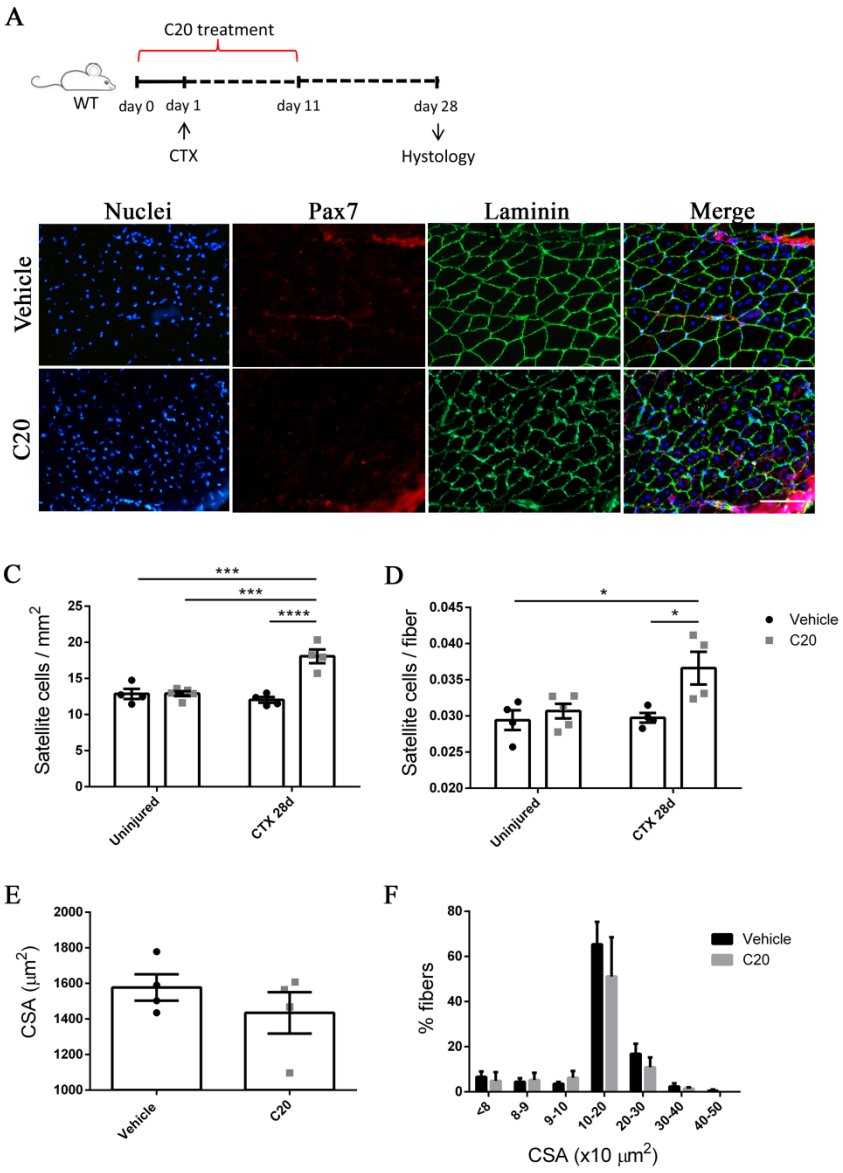

Figure 17: A: experimental plan. B: representative immunofluorescence pictures of WT GA sections 28 days after CTX injury, treated with C20 or

vehicle. Sections were stained for Pax7 (red) and Laminin (green). Nuclei were counterstained with Hoechst. Scale bar: 100μm. C: quantification of the number of SCs per mm^2 and D: number of SCs per fiber in uninjured and 28 day-injured GA muscle, in WT mice treated with C20 or vehicle. E: mean CSA and F: CSA distribution of muscle fibers in WT mice treated with C20 or vehicle, 28 days after injury. (C20 treated WT, n = 4 mice, Vehicle treated mice n = 4 mice). Error bars represent mean ± sem, *p < 0.05, ***p < 0.001, **** p < 0.0001 calculated by Two-way Anova with adjustment for multiple comparison test.

3.3.3 The number of quiescent satellite cells increases in PKCθ-/- mice after repeated injuries

It has been shown that satellite cell population is maintained after repeated traumas, thanks to their ability to self-renew. To investigate the behavior of PKCθ-/- satellite cells following repeated injury, we induced 3 CTX injuries in WT and PKCθ-/- GA muscles. The three injuries were performed 20 days apart from each other, and the muscles were analyzed 30 days after each injury, when regeneration is completed (Fig. 18A). As shown above, one month after the first injury we observed a 64% increase in the number of SCs/mm^2 in PKCθ-/- mice compared to WT. After 2 injuries this increase remained constant. However, one month after the third injury, while satellite cell number remained constant in WT mice, we observed an increase of 110% in the number of SCs/mm^2 in PKCθ-/- mice compared to WT mice. Also, the number of satellite cells per fiber was significantly higher. Notably, this increase was significant also comparing the number of satellite cells in PKCθ-/- mice after 2 injuries.
The CSA of regenerated muscle fibers 30 days after the third injury was similar between WT and PKCθ-/- mice (Figure 18E and F), suggesting that although more satellite cells undergo self-renewal in PKCθ-/- mice, the myogenic potential is maintained.

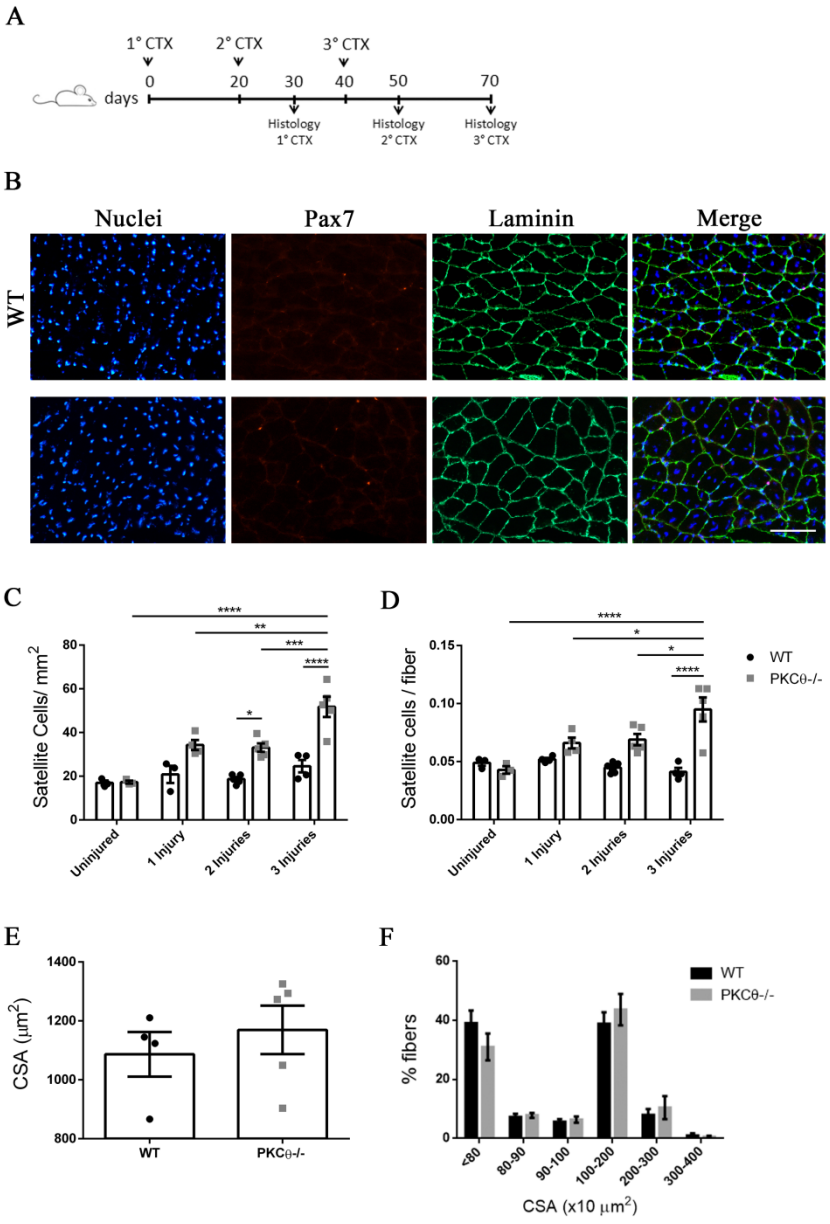
A
1° CTX
2° CTX
3° CTX
0
20
30
40
50
70
days
Histology 1° CTX
Histology 2° CTX
Histology 3° CTX
B
Nuclei
Pax7
Laminin
Merge
WT
C
Satellite Cells/ mm2
Uninjured
1 Injury
2 Injuries
3 Injuries
D
Satellite cells / fiber
WT
PKCθ-/-
E
CSA (μm2)
WT
PKCθ-/-
F
% fibers
WT
PKCθ-/-
<80
80-90
90-100
100-200
200-300
300-400
CSA (x10 μm2)

Figure 18: A: Experimental plan. B: representative immunofluorescence pictures of WT and PKCθ-/- GA sections 30 days after 3 CTX injury, scale bar: 100 μm. Sections were stained for Pax7 (red) and Laminin (green). Nuclei were counterstained with Hoechst. C: Quantification of the number of SCs/mm^2 D: and the number of SCs per fiber in uninjured GA from WT and PKCθ-/- mice, or after 1, 2 or 3 injuries. E: mean CSA of regenerated fibers 30 days after the third injury in WT and PKCθ-/- mice. F: Frequency of myofiber CSA from GA muscles of WT and PKCθ-/- mice, 30 days after the third injury. Error bars represent mean ± sem, *p < 0.05,**p < 0.01, ***p < 0.001, **** p < 0.0001 calculated by Two-way Anova with adjustment for multiple comparison test.

3.3.4 Notch1 expression is similar in satellite cells isolated from regenerating WT and PKCθ-/- muscles

Notch is considered one of the key factors regulating satellite cell self-renewal. In our preliminary results obtained in dystrophic mice, we found an increased Notch1 expression in satellite cells derived from mdx PKCθ-/- mice, compared to the ones isolated from mdx mice (Fiore P. et al. Int J Mol Sci. *Accepted*). To investigate whether the increased satellite cell self-renewal observed in PKCθ-/- mice depends on changes in Notch1, we analyzed its expression in satellite cells isolated from injured or uninjured muscles. We induced a CTX injury in WT and PKCθ-/- muscle, and we isolated satellite cells at 3, 5 and 7 days after injury, during the phases of satellite cell activation/proliferation and differentiation respectively. The results obtained show that Notch1 expression level in SCs isolated from WT and PKCθ-/- muscles either uninjured or injured, was similar (Figure 19A). The expression level of Delta1 and Jagged1, two of the Notch-1 ligands, was also analyzed in WT and PKCθ-/- uninjured or injured muscles. While Jagged1 expression was similar in uninjured muscle, it was significantly increased in PKCθ-/- muscle 3 and 7 days after CTX injury, compared to WT (Figure 19C). Delta1 expression, although increased in PKCθ-/- muscle after injury, did not reach a significant difference compared to WT instead (Figure

19B). These results together indicate that the increased satellite cell self-renewal observed in PKCθ-/- mice is not dependent on higher Notch1 expression. However, the increased expression of Notch ligands Delta1 and Jagged1 in injured in PKCθ-/- muscle, suggests that PKCθ affects Notch signalling, and further experiments are required to investigate this aspect.

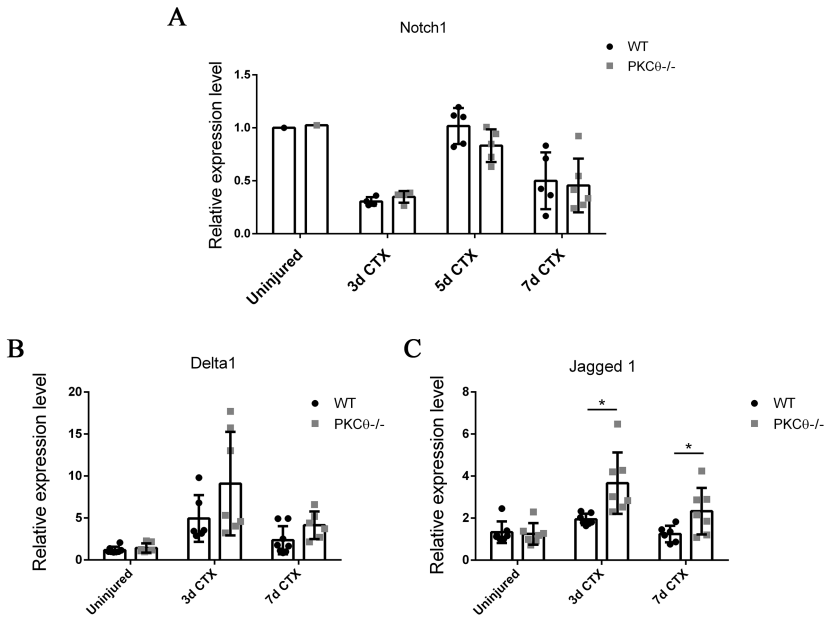

Figure 19: A: Notch1 expression level in satellite cells isolated from WT and PKCθ-/- uninjured TA muscles, or 3, 5 and 7 days after CTX injury, analyzed by RT-PCR. B: Delta1 and C: Jagged1 expression level in WT and PKCθ-/- uninjured TA muscles, or 3, 5 and 7 days after CTX injury, analyzed by RT-PCR. Error bars represent mean ± sem, *$p < 0.05$ calculated by Student's t-test.

3.4 Genetic ablation of PKCθ does not alter the inflammatory milieu after induction of acute injury

3.4.1 The quality and quantity of innate immune cells is not altered in PKCθ-/- regenerating muscle, in acute injury

While PKCθ plays an important role in effector T cell recruitment in the context of chronic muscle inflammation as we reported previously, less is known about its role in myeloid cell recruitment. Myeloid cells such as neutrophils and monocytes are the principal immune cell players during acute muscle injury. They influence satellite cell behavior by stimulating their activation, proliferation, and differentiation following injury. To understand whether PKCθ indirectly affects satellite cell behavior via immune cells, we analyzed myeloid cell infiltration in WT and PKCθ-/- injured muscles. Therefore, we injected WT and PKCθ-/- GA muscles with CTX, and we analyzed immune cell infiltration by flow cytometry, at 3 and 10 days after injury. At 3 days after injury, inflammatory monocytes invade the injured muscle and drive satellite cell activation and proliferation. At 10 days after injury, the switch of the pro-inflammatory M1 to the anti-inflammatory M2 macrophages stimulates satellite cell differentiation and muscle regeneration.

At 3 days after CTX, flow-cytometry analysis showed no significant difference in myeloid cell infiltration between WT and PKCθ-/- mice. Total number of infiltrating mononuclear cells, CD45+ cells, and CD11b+ cells, was similar between the two genotypes. M1 and M2 macrophages were identified as CD11b+ F4/80+ Ly6c-hi cells, and CD11b+ F4/80+ Ly6c-lo cells, respectively. As it is shown in figure 20, total number of M1 and M2 macrophages did not change significantly between WT and PKCθ-/- muscles. Within the M2 macrophage population, we analyzed the expression of CD206 marker, which was also similar.

At 10 days after CTX injury, total number of infiltrating inflammatory cells decreases in both WT and PKCθ-/- mice, compared to the 3 day-injured muscles. This evidence indicates that the inflammatory phase has been resolved and regeneration is ongoing. At this stage, total number of mononuclear cells, CD45+ cells, CD11b+ cells, M1 and M2 macrophages was similar in WT and PKCθ-/- mice. Also CD206 expression was similar (Figure 21).

Cytokines mediate the communication between immune and satellite cells. In particular, pro-inflammatory cytokines induce satellite cell activation and differentiation, and prevent their differentiation. Thus, we analyzed the expression level of some of the principal inflammatory cytokines from injured tibialis muscles, by rtPCR. The results obtained showed no significant difference in the expression level of TNF-α, IL-1β, and IL-6 between WT and PKCθ-/- mice, at 3 and 10 days after CTX injury (Figure 22). These results together confirm that PKCθ does not affect the inflammatory milieu during acute injury.

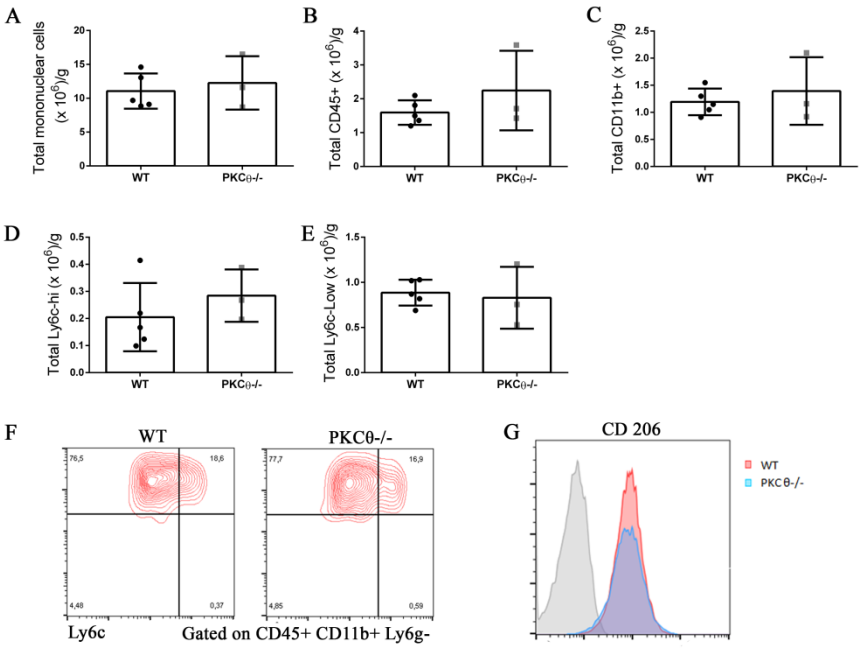

Figure 20: Flow Cytometry analysis of inflammatory cell infiltrate in WT and PKCθ-/- GA, 3 days after CTX injury. A: Total number of mononuclear cells, B: CD45+ cells, C: CD11b+ cells, D: Ly6c-hi+ cells and E: Ly6c-low+ cells, normalized on muscle mass 3 days after CTX injury in WT and PKCθ-/- GA. F: representative FACS plots showing M1 and M2 macrophage populations. G: histogram showing CD206 mean fluorescence in WT and PKCθ-/- GA 3d after CTX. Error bars represent mean ± sem.

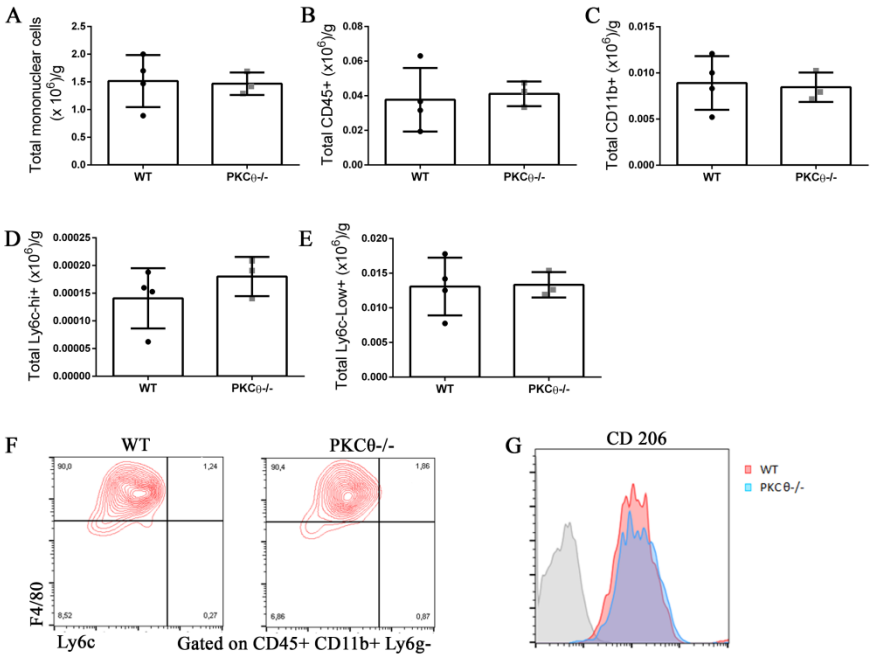

Figure 21: Flow Cytometry analysis of inflammatory cell infiltrate in WT and PKCθ-/- GA, 10 days after CTX injury. A: Total number of mononuclear cells, B: CD45+ cells, C: CD11b+ cells, D: Ly6c-hi+ cells and E: Ly6c-low+ cells, normalized on muscle mass 10 days after CTX injury in WT and PKCθ-/- GA. F: representative FACS plots showing M1 and M2 macrophage populations. G: histogram showing CD206 mean fluorescence in WT and PKCθ-/- GA 10d after CTX. Error bars represent mean ± sem.

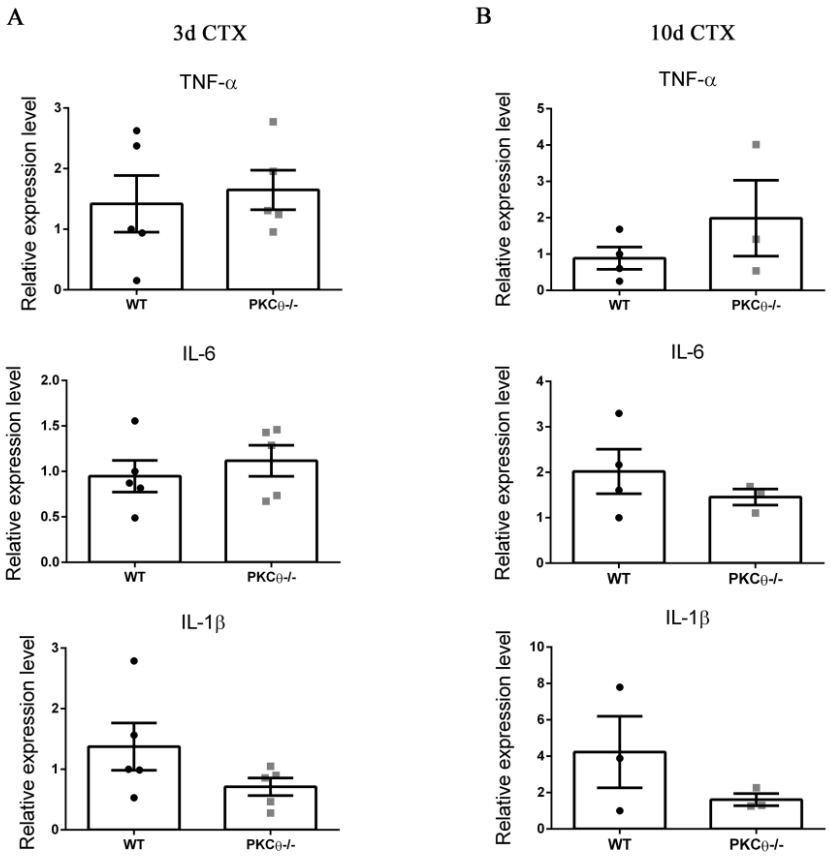

Figure 22: A: RT-PCR analysis of inflammatory cytokines TNF-α, IL-1β, and IL-6 at 3 days after CTX injury and B: 10 days after CTX injury, from total TA muscle RNA extract of WT and PKCθ-/- mice.

4. DISCUSSION

In the present study, we show that PKCθ is expressed in satellite cells. We found that a high level of PKCθ protein is expressed in recently activated satellite cells (i.e. freshly isolated cells). PKCθ expression then decreases in proliferating cells to increase again in differentiated cells. Interestingly, the ratio between the active phospho-PKCθ and total PKCθ is maximum in proliferating satellite cells. This result suggests that despite PKCθ expression decreases in proliferating satellite cells, its activity is high. Immunostaining with the phospho-PKCθ antibody allowed us to localyze the active form of the protein. Although it was not possible to identify phospho-PKCθ in sections to study its activation in quiescent satellite cells, we were able to stain cultured cells. In proliferating satellite cells, we detected phospho-PKCθ at the chromatin level during prophase. A previous study also observed PKCθ at the chromatin level in T cells. Sudha Rao's group showed that PKCθ can bind the promoter of genes and microRNA important for cytokine regulation, and induce their expression [79]. However, to the best of our knowledge, PKCθ was never observed in association with DNA in prophase. Therefore, it would be interesting to investigate in the future whether PKCθ is involved in the process of chromatin condensation. During metaphase in satellite cells, we showed that phospho-PKCθ moves to the centrosomes and partially to the mitotic spindle. During telophase and cytokinesis we detected phospho-PKCθ at the contractile ring of dividing satellite cells, which has never been reported previously. Abortive cytokinesis induces the formation of abnormal cells containing 2 or more nuclei [80]. We did not observe any aberrant cell division neither in PKCθ-/- satellite cells, nor in WT cells treated with C20. Although the role of PKCθ in cytokinesis is not known, based on our results we can speculate that PKCθ is not necessary for successful cytokinesis.

The localization of phospho-PKCθ to the mitotic machinery strongly suggested a role of this protein in the regulation of

satellite cell division. However, satellite cell proliferation was not affected by PKCθ absence *in vitro* and *in vivo*, after induction of CTX injury. Previously, Passalacqua et al. [81] provided evidence that PKCθ is recruited to the mitotic spindle of murine erythroleukaemia (MEL) cells and associates with centrosomes and kinetochore of dividing cells. Furthermore, in non-proliferating or differentiated MEL cells, PKCθ expression was down-regulated. Although the authors have not tested the effects of PKCθ ablation/ inhibition on MEL cell proliferation, they speculated a potential role of this protein in the regulation of cell growth and proliferation. In our study we found that PKCθ is highly expressed in satellite cells that have still to enter mitosis (i.e. freshly isolated satellite cells).Thus, PKCθ may be accumulated in non-dividing satellite cells, to be rapidly activated when cells enter mitosis. Another possibility is that PKCθ plays a yet unknown roles in satellite cells.

The localization of PKCθ to the centrosomes and mitotic spindle suggests a role of this protein in the mitotic spindle orientation and/or in the asymmetric segregation of cell fate determinants.

Indeed, we found that satellite cell symmetric division was significantly increased in cultured PKCθ-/- myofibers compared to WT. Furthermore, within the symmetric cell doublets, the number of Pax7+/MyoD- satellite cells was markedly higher compared to WT. This number remained elevated in PKCθ-/- myofibers even after 72h in culture, when satellite cells have proliferated. Together, these results indicate that lack of PKCθ stimulates satellite cell self-renewal. These observations were confirmed by the use of the pharmacological inhibitor of PKCθ, the C20. Treatment of cultured satellite cells with the C20 led to the expansion of the Pax7+MyoD- 'reserve cell' population. We also observed a reduction in cell fusion index after treatment with C20. This result is coherent with the fact that more cells underwent self-renewal. All of these effects were dose-dependent, with the highest dose of C20 used resembling the phenotype of knock out cells. Previously, we showed that PKCθ is required for the initial phase

of myoblast fusion, but not for the induction of terminal differentiation [52]. In this study, we showed that PKCθ is involved either directly or indirectly in the activation/ phosphorylation of Focal Adhesion Kinase (FAK). FAK, in turn, induces the expression of the profusion genes caveolin-3 and β1D integrin. Consequently, lack of PKCθ led to reduced fusion index in vitro, and slower muscle regeneration in vivo. In this study, no significant differences were observed between WT and PKCθ-/- satellite cells before fusion. However, the authors did not investigate the role of PKCθ on satellite cell self-renewal ability. The induction of FAK phosphorylation was associated with PKCθ activation and translocation to the cell membrane during myoblast differentiation. It is possible that according to the different dynamic subcellular localizations, PKCθ can play different roles. Thus, we speculate that when PKCθ is localized at the centrosome and mitotic spindle, it regulates division symmetry. Previous studies mostly done in Drosophila suggested that self-renewal regulators localize asymmetrically during mitosis, and they are inherited differently by the two daughter cells. This axis is used to distribute proteins that orient the mitotic spindle, and establish if the cell division will be planar or apico-basal. Par-3, Par-6 and aPKC form a complex involved in basically all the biological processes that require cell polarization. In embryonic neuroblasts, as well as in satellite cells, this complex localizes to the apical pole of the dividing stem cell, and direct mitotic spindle orientation. Par1 is a protein that participates in cellular polarity by phosphorylating Par3 and redistributing Par3-Par6-aPKC complex to the apical pole, opposite to where Par1 is localized. Par1 activity and localization is generally regulated by aPKC-dependent phosphorylation. However, it was demonstrated that also nPKCs can regulate Par1 activation and localization in HEK 293 cells, through PKD mediated phosphorylation [83]. PKCθ belongs to the family of nPKCs, and it is known to be an upstream regulator of PKD. Thus, it remains to be investigated whether PKCθ regulates Par1 phosphorylation and Par3 localization.

It was previously shown that Par1 absence in satellite cells leads to Par3 mislocalization. This causes an increase in satellite cell symmetric division, and an increase in the number of self-renewing cells. This phenotype resembles that of PKCθ-/- satellite cells. Knockdown of Par1 causes centrosome multipolarity and abnormal cell division [84]. However, PKCθ-/- satellite cells displayed a normal mitotic spindle formation observed by immunofluorescence analysis for tubulin.

The *in vivo* analysis confirmed that satellite cell self-renewal ability is increased in PKCθ-/- mice. After the induction of muscle injury, the number of satellite cells going back to quiescence is increased of 65% in PKCθ-/- mice, compared to WT . Also the pharmacological inhibition of PKCθ with C20 inhibitor leads to similar results after injury. In this case, quiescent satellite cell number was increased by 50% compared to vehicle treated mice. The lower percentage compared to PKCθ-/- mice could depend on the dose of C20 used, which probably did not result in the complete inhibition of the protein function. Indeed, we used the lowest dose of C20 *in vivo* that was sufficient to reduce T cell function significantly. As observed in cultured cells treated with C20, the effect on self-renewal is dose-dependent. Thus, it is possible that increasing the dose of C20 *in vivo* we can increase the number of self-renewing satellite cells. Notably, a 10-day treatment with C20 during the first phase of regeneration was sufficient to observe the increase of the quiescent satellite cell pool. This result suggests that PKCθ inhibitor treatment can be effective even when administered for a short period of time.

PKCθ could be a promising target for the treatment of pathological conditions where satellite cells show an enhanced myogenic commitment, such as aging. Satellite cell number and function decline in late adulthood and muscle gradually loses its regenerative ability. The functional decline is due to modifications in the satellite cell niche, such as deregulations in Wnt, Notch, and TGFβ pathways. Moreover, fibrosis and inflammation increase with age, negatively affecting regeneration [85]. Intrinsic defects in

satellite cells from aged mice involve the upregulation of p-38 and JAK-STAT pathway, which result in the loss of self-renewal ability and regeneration.
Treatment with p-38 inhibitors or JAK-STAT inhibitors led to the rescue of self-renewal ability and improved regeneration in aged mice [86]. Of note, it would be interesting to investigate whether PKCθ expression/phosphorylation increases in aged satellite cells. In this case, PKCθ can be targeted to rescue aged satellite cell defects.
We showed that the induction of repeated injuries in PKCθ-/- muscle leads to a progressive increase in the number of quiescent satellite cells, without adverse effects on the regenerative ability. This result suggests that PKCθ inhibition may counteract satellite cell loss by limiting the number of cells committed to differentiation, in aged mice. In mdx PKCθ-/- mice, we observed that the number of satellite cells increases at 12 months of age compared to mdx (Fiore P. et al. Int J Mol Sci. *Accepted*). Although 12-month-old mice are not considered aged, we can speculate that this increased number of satellite cells is maintained even in older mice.
Overall our results show that PKCθ plays a direct role in SC activity.
We previously demonstrated that PKCθ is a promising anti-inflammatory target in the context of muscular dystrophy. PKCθ inhibition targets effector T cells and ameliorates inflammation and necrosis during the acute phase of the disease [72], [73]. Here we show that PKCθ can also be directly targeted to improve and maintain the satellite cell pool.

5. MATERIALS AND METHODS

5.1 Animal models

PKCθ-/- mice (C57BL/6J background) were provided by Dan Littman (New York University, New York). In these mice, the gene encoding PKCθ Is inactivated in all cells of the body, as previously described [66].
C57BL/6J control mice were purchased from Jackson laboratory. The animals were housed in the Histology Department–accredited animal facility. All the procedures were approved by the Italian Ministry for Health and were conducted according to the U.S. National Institutes of Health (NIH) guidelines.

5.2 Cardiotoxin injury

Before Cardiotoxin, mice were anesthetized by intra-muscular injection of zoletil (50/50 mg/ml) and rompun (20 mg/ml). Cardiotoxin injury was performed by injecting 20 µl of Cardiotoxin from Naja Pallida (10 mMol in H2O, Latoxan L8102) with two injections of 10 µl each, in two different areas of the GA muscle using a 30 Gauge microsyringe.

5.3 Single myofiber isolation and culture

Single myofibers were isolated from EDL muscles of 4-8-week-old mice. EDL muscles were dissected from tendon to tendon and incubated in DMEM (Sigma-Aldrich D6546) containing 0.2% collagenase I (Sigma-Aldrich C01130) for 45 minutes. Myofibers were then dissociated by gentle flushing with a glass pipette, in a dish containing DMEM 1% penicillin streptomycin (Sigma-Aldrich P0781). Then myofibers were washed 3 times in DMEM 1% penicillin-streptomycin, and were left for 1h in the last washing dish. Myofibers were then cultured in suspension in Horse Serum (Gibco, 26050088) coated dishes, in high glucose DMEM

containing 1% penicillin-streptomycin, 1% Chick Embryo Extract (CEE, produced in the lab), 20% FBS (Sigma-Aldrich F7524).

5.4 Satellite cell isolation and culture

SCs were prepared from hind-limb muscles of 4-8 week old mice. Muscles were dissected with scissors and finely diced with a scalpel. For enzymatic digestion, muscles were incubated in Collagenase type II (Sigma-Aldrich C6885) 0.4 mg/ml in PBS (Sigma-Aldrich D8537), for 45 min in shaking water bath at 37°C. A second digestion was performed in 1 mg/ml of Collagene/Dispase (Roche 11097113001) in PBS Calcium-Magnesium free (Sigma-Aldrich D8537), for 30 min at 37°C. Digestion was then blocked with 10 ml of FBS 10% in DMEM. The digested muscle was then passed through 70µm cell strainer first, and 40µm cell strainer then, to remove debris. Next, satellite cell purification was performed by using SC Isolation Kit (Miltenyi Biotech 130-104-268). For magnetic labeling the cells were resuspended in 80 µl buffer (PBS pH 7.2, 0.5% FBS, 2mM EDTA) and 20 µl of Satellite Cell Isolation Kit per gram of tissue. The cells were then incubated for 15 min at 4°C. Following the incubation, volume was adjusted to 500 µl with the buffer, and cell suspension was passed through a LS column placed in a magnetic field of a MACS Separator. Flow-through was collected, and the column was washed twice with 1 ml of buffer. Unlabeled cells were collected with flow-through of the previous step. Cells were then counted, washed, resuspended in growth medium (GM) and plated. GM contained DMEM 20% HS, 3% Embryo Extract. Differentiation medium (DM) contained DMEM 5% HS, 1% CEE.

5.5 Immunofluorescence analysis

For immunofluorescence on sections, 8 µm muscle cryosections were fixed in 4% PFA (Sigma-Aldrich HT5011) for 10 min RT, and then permeabilized in cold methanol for 6 min at -20°C. Next,

antigen retrieval was performed in Citric Acid 0.01M pH 6, for 10 min at 90°C. Sections were then blocked in BSA (Sigma-Aldrich A2058) 4%, Goat Serum (Sigma-Aldrich G9023) 5% for 30 min RT. Sections were then incubated in M.O.M. Mouse Ig Blocking reagent (Vector Laboratories MKB-2213) for 1h RT, and then in M.O.M. Diluent for 5 min. Subsequently, sections were incubated with primary mouse anti-Pax7 antibody (Developmental Studies Hybridoma Bank) diluted 1:10 in M.O.M. Diluent, for 30 min RT. Sections were then incubated with rabbit anti-laminin (Sigma-Aldrich L9393) 1:200 diluted in BSA 4%, and biotin anti-mouse 1:1000 (BioLegend 405303) O/N at 4°C in humid chamber. The next day sections were incubated in secondary antibodies Streptavidin-Cy3 1:500 (BioLegend 405215) and goat anti rabbit IgG Alexa Fluor 488 1:1000 (Abcam ab150077). Nuclei were counterstained with Hoechst.

For immunofluorescence on cultured cells, the cells were fixed for 10 min with PFA 4% RT, and then permeabilized in cold methanol for 6 min at -20°C. Next, cells were blocked in BSA (Sigma-Aldrich A2058) 4%, Goat Serum (Sigma-Aldrich G9023) 5% for 30 min RT. The cells were then incubated over-night with primary anti-Pax7 antibody 1:10 (Developmental Studies Hybridoma Bank), anti-MyoD antibody 1:50 (Santa Cruz C20: sc-304), anti phospho-PKCθ antibody 1:50 (Thr538-Cell Signaling 9377), and anti-α-tubulin 1:2000 (Sigma-Aldrich T5168). Primary antibodies were diluted in BSA 1% PBS. The next day the cells were washed three times with PBS and incubated with secondary antibodies diluted in BSA 1% PBS, for 1h RT in dark. Secondary antibodies used were: goat anti rabbit IgG Alexa Fluor 488 1:1000 (Abcam ab150077), and goat anti mouse IgG Alexa Fluor 555 1:1000 (Thermo-Fisher A-21422). Nuclei were counterstained with Hoechst.

For myofiber staining, myofibers were fixed in PFA 4% for 5 min RT, permeabilized in cold methanol -20°C for 6 min, and

incubated in Glycin 1M for 10 min RT to reduce background. Blocking was performed in BSA 4%, Goat Serum 5% for 30 min RT. Primary antibodies mouse anti Pax7 and rabbit anti-MyoD 1:50 (Santa Cruz C20: sc-304) were incubated O/N at 4°C in humid chamber. The next day myofibers were incubated for 1h RT in biotin anti-mouse and subsequently in secondary antibodies goat anti rabbit Alexa Fluor 488 and Streptavidin Cy3 for 1h RT, at the concentration listed before. Nuclei were counterstained with Hoechst and Topro3. Samples were analyzed under an epifluorescence Zeiss Axioskop 2 Plus microscope.

5.6 CSA analysis

Muscle fiber CSA was analyzed by using ImageJ software from Rasband, W.S., ImageJ**,** U. S. National Institutes of Health, Bethesda, Maryland, USA.

5.7 Western Blot

Satellite cells were homogenized in ice-cold buffer containing 20 mMTris (pH 7.5), 2 mM EDTA, 2 mM EGTA, 250 mM sucrose, 5 mM DTT, 200 mg/ml leupeptin, 10 mg/ml Trasylol, 1 mM PMSF, and 0.1% Triton X-100 and then disrupted by sonication. The homogenate was then incubated for 30 min at 4°C in rotation, then centrifuged at 12,000g for 10 min at 4°C. The pellet was discarded. Protein determination was performed by using the Comassie Plus protein assay reagent (Pierce, Rockford, IL), according to the manufacturer's instruction. Proteins from each sample were loaded onto 10% SDS-polyacrylamide gels and transferred to a nitrocellulose membrane (Schleicher and Schuell, Dassel, Germany). The membranes were incubated with anti-PKCθ (Cell Signaling #2059) and anti phospho-PKCθ (Thr538-Cell Signaling #9377) primary antibodies 1:1000 diluted in BSA 5% in TBS 1% tween. HRP-conjugated goat anti–rabbit IgG 1:5000 diluted in BSA 5% in TBS 1% tween (Bethyl Laboratories A120-101P) was used as secondary antibody, and immunoreactive bands were

detected using ECL solution, according to the manufacturer's instructions. Chemiluminescent signals were acquired by ChemiDoc MP Imaging System (Bio-Rad). Densitometric analysis was performed using ImageJ software. Proteins were normalized to GAPDH (Santa Cruz 6C5: sc-32233).

5.8 Cell isolation and cytofluorimetric analysis

To prepare single cell suspension, muscles were dissected from mice and finely minced with a scalpel in a dish containing DMEM. Next, minced muscles were digested in a solution of Collagenase type IV (Worthington Cat. No. 9001-12-1**)** 1 mg/ml in DMEM, (10 ml/g of muscle) for 1h 30 min in shaking water bath at 37°C. Then, digested muscles were passed through a 70 µm cell strainer first and then through a 40 µm cell strainer, to exclude cell debris. Muscle single cell suspension was then resuspended in FACS buffer (PBS 1% FBS) and incubated 30 min on ice with the following antibodies: anti-CD45 (Biolegend, clone 30-F11, 1:6000), anti-Ly6G (eBioscience, clone 1A8 and clone RB6-8C5, 1:3000), anti-Ly6c (Biolegend, clone HK1.4, 1:100), anti-F4/80 (Biolegend, clone BM8, 1:1000), anti-CD206 (MMR) (Biolegend, clone C068C2, 1:50), anti-CD11b (Biolegend, clone M1/70, 1:3000). Cell viability was assessed with 4',6-diamidino-2-phenylindole dilactate (DAPI) (BioLegend, 422801). Compensation was set using the ABC compensation beads kit (Thermo Fisher, Eugene, OR, USA; A10389 and A10344). Samples were processed using a Dako CyAn ADP flow cytometer and acquired data were analyzed using FlowJo software version 10 (FlowJo LLC, Ashland, OR, USA).

5.9 CFSE analysis

Isolated SCs were stained with CFSE (ThermoFisher Scientific. C34554) 5 µm for 20' at 37°C in dark prior to culture. After 72h in culture in GM SCs were detached with accutase and fluorescence

was analyzed with a CyAn ADP (DAKO). Acquired data were analyzed using FlowJo software version 10.

5.10 RNA isolation and Real Time PCR analysis

For RNA isolation, the cells were collected in TRI reagent (Sigma-Aldrich T9424). For RNA preparation from muscle, the muscles were homogenized in TissueLyser (Quiagen) in the presence of TRI reagent. Next, homogenized tissue was syringed 3 times with a 21G needle syringe. Then, samples were centrifuged at 12.000 g for 10 minutes at 4°C and the pellet was discarded. For every ml of TRI reagent used, 200ul of Chloroform were added. After centrifugation for 15 minutes at 12000 g, the aqueous phase containing the RNA was recovered. For every ml of TRI reagent used, 500ul of isopropanol were added to the aqueous phase. After 10 minutes of incubation at RT and centrifugation for 10 minutes at 12000 g, the RNA precipitates. The RNA in aqueous phase was washed with a solution of cold 75% Ethanol in water and then resuspended in RNAse and DNAse free water. RNA was retrotranscribed to cDNA using the SensiFAST™ cDNA Synthesis Kit (Bioline Cat. No. BIO-65054). PCR amplification was performed using the SensiMix™ SYBR® Low-ROX Kit (Bioline QT625-05), following the manufacturer's protocol. Data analysis was performed using 7500 Software v2.0.6 provided by Applied Biosystems. Data are expressed as fold-change in expression levels. Relative expression levels were normalized to GAPDH mRNA. The primers used are listed below.

GAPDH For: Rev:	 5’ ACCCAGAAGACTGTGGATGG 3’ 5’ CACATTGGGGGTAGGAACAC 3’
IL-6 For: Rev:	 5’ ATGAAGTTCCTCTCTGCAAGAGACT 3’ 5’ CACTAGGTTTGCCGAGTAGATCTC 3’
TNF-α For: Rev:	 5’ ATGATCCGCGACGTGAA 3’ 5’ AGGGAGGCCATTTGGGAA 3’
PKCθ For: Rev:	 5’ CCTACTGCGCTGTGCTTGTC 3’ 5’ GGGAGTAGAGTTCCACGGTTG 3’
Notch1 For: Rev:	 5’ GGTCGCAACTGTGAGAGTGA 3’ 5’ TTGCTGGCACATTCATTGAT 3’
Delta1 For: Rev:	 5’ CCGGCTGAAGCTACAGAAAC 3’ 5’ GAAAGTCCGCCTTCTTGTTG 3’
Jagged1 For: Rev:	 5’ ATCGTGCTGCCAGTTT 3’ 5’ GGTCACGCGGGATACT 3’

IL-1β For: Rev:	 5’ AGTGTGGATCCCAAGCA 3’ 5’ CACTGTTGTTTCCCAGGA 3’

5.11 Statistical analysis

All statistical analyses were performed using GraphPad Prism software version 6. Quantitative data are presented as means ± SEM of at least three experiments. Statistical analysis to determine significance was performed using Student’s t tests or Anova test. Differences were considered to be statistically significant at the $p < 0.05$ level

6. REFERENCES

[1] A. Mauro, "SATELLITE CELL OF SKELETAL MUSCLE FIBERS," *J. Cell Biol.*, vol. 9, no. 2, pp. 493–495, Feb. 1961.

[2] F. Relaix, D. Rocancourt, A. Mansouri, and M. Buckingham, "Divergent functions of murine Pax3 and Pax7 in limb muscle development.," *Genes Dev.*, vol. 18, no. 9, pp. 1088–105, May 2004.

[3] V. F. Gnocchi, R. B. White, Y. Ono, J. A. Ellis, and P. S. Zammit, "Further characterisation of the molecular signature of quiescent and activated mouse muscle satellite cells.," *PLoS One*, vol. 4, no. 4, p. e5205, Apr. 2009.

[4] M. T. Tierney and A. Sacco, "Satellite Cell Heterogeneity in Skeletal Muscle Homeostasis," *Trends Cell Biol.*, vol. 26, no. 6, pp. 434–444, Jun. 2016.

[5] H. Yin, F. Price, and M. A. Rudnicki, "Satellite Cells and the Muscle Stem Cell Niche," *Physiol. Rev.*, vol. 93, no. 1, pp. 23–67, Jan. 2013.

[6] A. E. Almada and A. J. Wagers, "Molecular circuitry of stem cell fate in skeletal muscle regeneration, ageing and disease," *Nat. Rev. Mol. Cell Biol.*, vol. 17, no. 5, pp. 267–279, May 2016.

[7] I. M. Conboy and T. A. Rando, "The regulation of Notch signaling controls satellite cell activation and cell fate determination in postnatal myogenesis.," *Dev. Cell*, vol. 3, no. 3, pp. 397–409, Sep. 2002.

[8] Y. Wen, P. Bi, W. Liu, A. Asakura, C. Keller, and S. Kuang, "Constitutive Notch Activation Upregulates Pax7 and Promotes the Self-Renewal of Skeletal Muscle Satellite Cells," *Mol. Cell. Biol.*, vol. 32, no. 12, p. 2300, 2012.

[9] S. Fukada *et al.*, "Molecular Signature of Quiescent Satellite Cells in Adult Skeletal Muscle," *Stem Cells*, vol. 25, no. 10, pp. 2448–2459, Oct. 2007.

[10] H. Jockusch and S. Voigt, "Migration of adult myogenic

precursor cells as revealed by GFP/nLacZ labelling of mouse transplantation chimeras.," *J. Cell Sci.*, vol. 116, no. Pt 8, pp. 1611–6, Apr. 2003.

[11] L. A. Sabourin, A. Girgis-Gabardo, P. Seale, A. Asakura, and M. A. Rudnicki, "Reduced differentiation potential of primary MyoD-/- myogenic cells derived from adult skeletal muscle.," *J. Cell Biol.*, vol. 144, no. 4, pp. 631–43, Feb. 1999.

[12] Y. Cao *et al.*, "Global and gene-specific analyses show distinct roles for Myod and Myog at a common set of promoters.," *EMBO J.*, vol. 25, no. 3, pp. 502–11, Feb. 2006.

[13] Z. Wu *et al.*, "p38 and extracellular signal-regulated kinases regulate the myogenic program at multiple steps.," *Mol. Cell. Biol.*, vol. 20, no. 11, pp. 3951–64, Jun. 2000.

[14] A. Mal, M. Sturniolo, R. L. Schiltz, M. K. Ghosh, and M. L. Harter, "A role for histone deacetylase HDAC1 in modulating the transcriptional activity of MyoD: inhibition of the myogenic program," *EMBO J.*, vol. 20, no. 7, pp. 1739–1753, Apr. 2001.

[15] J. Lu, T. A. McKinsey, C. L. Zhang, and E. N. Olson, "Regulation of skeletal myogenesis by association of the MEF2 transcription factor with class II histone deacetylases.," *Mol. Cell*, vol. 6, no. 2, pp. 233–44, Aug. 2000.

[16] M. Horak, J. Novak, and J. Bienertova-Vasku, "Muscle-specific microRNAs in skeletal muscle development," *Dev. Biol.*, vol. 410, no. 1, pp. 1–13, Feb. 2016.

[17] C. A. Collins *et al.*, "Stem cell function, self-renewal, and behavioral heterogeneity of cells from the adult muscle satellite cell niche.," *Cell*, vol. 122, no. 2, pp. 289–301, Jul. 2005.

[18] A. Sacco, R. Doyonnas, P. Kraft, S. Vitorovic, and H. M. Blau, "Self-renewal and expansion of single transplanted muscle stem cells," *Nature*, vol. 456, no. 7221, pp. 502–506,

Nov. 2008.
[19] S. Kuang, K. Kuroda, F. Le Grand, and M. A. Rudnicki, "Asymmetric Self-Renewal and Commitment of Satellite Stem Cells in Muscle," *Cell*, vol. 129, no. 5, pp. 999–1010, Jun. 2007.
[20] F. Le Grand, A. E. Jones, V. Seale, A. Scimè, and M. A. Rudnicki, "Wnt7a activates the planar cell polarity pathway to drive the symmetric expansion of satellite stem cells.," *Cell Stem Cell*, vol. 4, no. 6, pp. 535–47, Jun. 2009.
[21] F. D. Price *et al.*, "Inhibition of JAK-STAT signaling stimulates adult satellite cell function," *Nat. Med.*, vol. 20, no. 10, pp. 1174–1181, Oct. 2014.
[22] K. Day, G. Shefer, J. B. Richardson, G. Enikolopov, and Z. Yablonka-Reuveni, "Nestin-GFP reporter expression defines the quiescent state of skeletal muscle satellite cells.," *Dev. Biol.*, vol. 304, no. 1, pp. 246–59, Apr. 2007.
[23] V. Shinin, B. Gayraud-Morel, and S. Tajbakhsh, "Template DNA-Strand Co-Segregation and Asymmetric Cell Division in Skeletal Muscle Stem Cells," in *Methods in molecular biology (Clifton, N.J.)*, vol. 482, 2009, pp. 295–317.
[24] A. Troy, A. B. Cadwallader, Y. Fedorov, K. Tyner, K. K. Tanaka, and B. B. Olwin, "Coordination of Satellite Cell Activation and Self-Renewal by Par-Complex-Dependent Asymmetric Activation of p38α/β MAPK," *Cell Stem Cell*, vol. 11, no. 4, pp. 541–553, Oct. 2012.
[25] J. A. Knoblich, "Asymmetric cell division: recent developments and their implications for tumour biology," *Nat. Rev. Mol. Cell Biol.*, vol. 11, no. 12, pp. 849–860, Dec. 2010.
[26] S. Goulas, R. Conder, and J. A. Knoblich, "The Par Complex and Integrins Direct Asymmetric Cell Division in Adult Intestinal Stem Cells," *Cell Stem Cell*, vol. 11, no. 4, pp. 529–540, Oct. 2012.
[27] N. A. Dumont *et al.*, "Dystrophin expression in muscle stem cells regulates their polarity and asymmetric division.," *Nat.*

Med., vol. 21, no. 12, pp. 1455–63, Dec. 2015.
[28] R. A. Neumüller and J. A. Knoblich, "Dividing cellular asymmetry: asymmetric cell division and its implications for stem cells and cancer.," *Genes Dev.*, vol. 23, no. 23, pp. 2675–99, Dec. 2009.
[29] E. P. Hoffman, R. H. Brown, and L. M. Kunkel, "Dystrophin: The protein product of the duchenne muscular dystrophy locus," *Cell*, vol. 51, no. 6, pp. 919–928, Dec. 1987.
[30] N. A. Dumont and M. A. Rudnicki, "Targeting muscle stem cell intrinsic defects to treat Duchenne muscular dystrophy," *npj Regen. Med.*, vol. 1, no. 1, p. 16006, Dec. 2016.
[31] L. Heslop, J. E. Morgan, and T. A. Partridge, "Evidence for a myogenic stem cell that is exhausted in dystrophic muscle.," *J. Cell Sci.*, vol. 113 (Pt 12), pp. 2299–308, Jun. 2000.
[32] A. Sacco *et al.*, "Short telomeres and stem cell exhaustion model Duchenne muscular dystrophy in mdx/mTR mice.," *Cell*, vol. 143, no. 7, pp. 1059–71, Dec. 2010.
[33] C. Jiang, Y. Wen, K. Kuroda, K. Hannon, M. A. Rudnicki, and S. Kuang, "Notch signaling deficiency underlies age-dependent depletion of satellite cells in muscular dystrophy.," *Dis. Model. Mech.*, vol. 7, no. 8, pp. 997–1004, Aug. 2014.
[34] J. G. Tidball, "Regulation of muscle growth and regeneration by the immune system," *Nat. Rev. Immunol.*, vol. 17, no. 3, pp. 165–178, Mar. 2017.
[35] J. G. Tidball and S. A. Villalta, "Regulatory interactions between muscle and the immune system during muscle regeneration," *Am. J. Physiol. Integr. Comp. Physiol.*, vol. 298, no. 5, pp. R1173–R1187, May 2010.
[36] R. A. Collins and M. D. Grounds, "The role of tumor necrosis factor-alpha (TNF-alpha) in skeletal muscle regeneration. Studies in TNF-alpha(-/-) and TNF-alpha(-/-)/LT-alpha(-/-) mice.," *J. Histochem. Cytochem.*, vol. 49, no.

8, pp. 989–1001, Aug. 2001.
[37] M. Cheng, M.-H. Nguyen, G. Fantuzzi, and T. J. Koh, "Endogenous interferon-gamma is required for efficient skeletal muscle regeneration.," *Am. J. Physiol. Cell Physiol.*, vol. 294, no. 5, pp. C1183-91, May 2008.
[38] F. O. Martinez and S. Gordon, "The M1 and M2 paradigm of macrophage activation: time for reassessment.," *F1000Prime Rep.*, vol. 6, p. 13, Mar. 2014.
[39] D. Burzyn *et al.*, "A special population of regulatory T cells potentiates muscle repair.," *Cell*, vol. 155, no. 6, pp. 1282–95, Dec. 2013.
[40] G. L. WARREN *et al.*, "Physiological role of tumor necrosis factor α in traumatic muscle injury," *FASEB J.*, vol. 16, no. 12, pp. 1630–1632, Oct. 2002.
[41] S.-E. Chen *et al.*, "Role of TNF-α signaling in regeneration of cardiotoxin-injured muscle," *Am. J. Physiol. Physiol.*, vol. 289, no. 5, pp. C1179–C1187, Nov. 2005.
[42] R. C. J. Langen, J. L. J. Van Der Velden, A. M. W. J. Schols, M. C. J. M. Kelders, E. F. M. Wouters, and Y. M. W. Janssen-Heininger, "Tumor necrosis factor-alpha inhibits myogenic differentiation through MyoD protein destabilization.," *FASEB J.*, vol. 18, no. 2, pp. 227–37, Feb. 2004.
[43] D. C. Guttridge, C. Albanese, J. Y. Reuther, R. G. Pestell, and A. S. Baldwin, "NF-kappaB controls cell growth and differentiation through transcriptional regulation of cyclin D1.," *Mol. Cell. Biol.*, vol. 19, no. 8, pp. 5785–99, Aug. 1999.
[44] P. Muñoz-Cánoves, C. Scheele, B. K. Pedersen, and A. L. Serrano, "Interleukin-6 myokine signaling in skeletal muscle: a double-edged sword?," *FEBS J.*, vol. 280, no. 17, pp. 4131–48, Sep. 2013.
[45] M. Cheng, M.-H. Nguyen, G. Fantuzzi, and T. J. Koh, "Endogenous interferon-γ is required for efficient skeletal muscle regeneration," *Am. J. Physiol. Physiol.*, vol. 294, no.

5, pp. C1183–C1191, May 2008.
[46] P. Londhe and J. K. Davie, "Gamma interferon modulates myogenesis through the major histocompatibility complex class II transactivator, CIITA.," *Mol. Cell. Biol.*, vol. 31, no. 14, pp. 2854–66, Jul. 2011.
[47] B. Deng, M. Wehling-Henricks, S. A. Villalta, Y. Wang, and J. G. Tidball, "IL-10 triggers changes in macrophage phenotype that promote muscle growth and regeneration.," *J. Immunol.*, vol. 189, no. 7, pp. 3669–80, Oct. 2012.
[48] J. Tonkin *et al.*, "Monocyte/Macrophage-derived IGF-1 Orchestrates Murine Skeletal Muscle Regeneration and Modulates Autocrine Polarization," *Mol. Ther.*, vol. 23, no. 7, pp. 1189–1200, Jul. 2015.
[49] V. Marrocco, P. Fiore, L. Madaro, A. Crupi, B. Lozanoska-Ochser, and M. Bouché, "Targeting PKCθ in skeletal muscle and muscle diseases: good or bad?: Table 1," *Biochem. Soc. Trans.*, vol. 42, no. 6, pp. 1550–1555, Dec. 2014.
[50] F. Zappelli *et al.*, "The Inhibition of Differentiation Caused by TGFβ in Fetal Myoblasts Is Dependent upon Selective Expression of PKCθ: A Possible Molecular Basis for Myoblast Diversification during Limb Histogenesis," *Dev. Biol.*, vol. 180, no. 1, pp. 156–164, Nov. 1996.
[51] G. Messina *et al.*, "Nfix Regulates Fetal-Specific Transcription in Developing Skeletal Muscle," *Cell*, vol. 140, no. 4, pp. 554–566, Feb. 2010.
[52] L. Madaro *et al.*, "PKCθ signaling is required for myoblast fusion by regulating the expression of caveolin-3 and β1D integrin upstream focal adhesion kinase.," *Mol. Biol. Cell*, vol. 22, no. 8, pp. 1409–19, Apr. 2011.
[53] J. S. Marino *et al.*, "Suppression of protein kinase C theta contributes to enhanced myogenesis in vitro via IRS1 and ERK1/2 phosphorylation.," *BMC Cell Biol.*, vol. 14, p. 39, Sep. 2013.
[54] M.-X. Li *et al.*, "The role of the theta isoform of protein

kinase C (PKC) in activity-dependent synapse elimination: evidence from the PKC theta knock-out mouse in vivo and in vitro.," *J. Neurosci.*, vol. 24, no. 15, pp. 3762–9, Apr. 2004.

[55] N. Besalduch *et al.*, "Transmitter release in the neuromuscular synapse of the protein kinase C theta-deficient adult mouse," *J. Comp. Neurol.*, vol. 519, no. 5, pp. 849–855, Apr. 2011.

[56] L. Madaro, V. Marrocco, S. Carnio, M. Sandri, and M. Bouché, "Intracellular signaling in ER stress-induced autophagy in skeletal muscle cells," *FASEB J.*, vol. 27, no. 5, pp. 1990–2000, May 2013.

[57] G. M. Camerino *et al.*, "Protein kinase C theta (PKCθ) modulates the ClC-1 chloride channel activity and skeletal muscle phenotype: a biophysical and gene expression study in mouse models lacking the PKCθ.," *Pflugers Arch.*, vol. 466, no. 12, pp. 2215–28, Dec. 2014.

[58] E. Y. Zhang, K.-F. Kong, and A. Altman, "The yin and yang of protein kinase C-theta (PKCθ): a novel drug target for selective immunosuppression.," *Adv. Pharmacol.*, vol. 66, pp. 267–312, 2013.

[59] Z.-B. Xu *et al.*, "Catalytic domain crystal structure of protein kinase C-theta (PKCtheta).," *J. Biol. Chem.*, vol. 279, no. 48, pp. 50401–9, Nov. 2004.

[60] G. Baier *et al.*, "Molecular cloning and characterization of PKC theta, a novel member of the protein kinase C (PKC) gene family expressed predominantly in hematopoietic cells.," *J. Biol. Chem.*, vol. 268, no. 7, pp. 4997–5004, Mar. 1993.

[61] Y. Liu, C. Graham, V. Parravicini, M. J. Brown, J. Rivera, and S. Shaw, "Protein kinase C theta is expressed in mast cells and is functionally involved in Fcepsilon receptor I signaling.," *J. Leukoc. Biol.*, vol. 69, no. 5, pp. 831–40, May 2001.

[62] Y. M. Vyas *et al.*, "Spatial organization of signal

transduction molecules in the NK cell immune synapses during MHC class I-regulated noncytolytic and cytolytic interactions.," *J. Immunol.*, vol. 167, no. 8, pp. 4358–67, Oct. 2001.

[63] S. Osada, K. Mizuno, T. C. Saido, K. Suzuki, T. Kuroki, and S. Ohno, "A new member of the protein kinase C family, nPKC theta, predominantly expressed in skeletal muscle.," *Mol. Cell. Biol.*, vol. 12, no. 9, pp. 3930–8, Sep. 1992.

[64] C. Serra *et al.*, "Transgenic mice with dominant negative PKC-theta in skeletal muscle: a new model of insulin resistance and obesity.," *J. Cell. Physiol.*, vol. 196, no. 1, pp. 89–97, Jul. 2003.

[65] A. Zanin-Zhorov, M. L. Dustin, and B. R. Blazar, "PKC-θ and the immunological synapse: mechanisms and implications," *Trends Immunol.*, vol. 32, no. 8, p. 358, Aug. 2011.

[66] Z. Sun *et al.*, "PKC-θ is required for TCR-induced NF-κB activation in mature but not immature T lymphocytes," *Nature*, vol. 404, no. 6776, pp. 402–407, Mar. 2000.

[67] N. Coudronniere, "NF-kappa B activation induced by T cell receptor/CD28 costimulation is mediated by protein kinase C-theta," *Proc. Natl. Acad. Sci.*, vol. 97, no. 7, pp. 3394–3399, Mar. 2000.

[68] N. N. Berg-Brown *et al.*, "PKCtheta signals activation versus tolerance in vivo.," *J. Exp. Med.*, vol. 199, no. 6, pp. 743–52, Mar. 2004.

[69] S. Gupta, S. Manicassamy, C. Vasu, A. Kumar, W. Shang, and Z. Sun, "Differential requirement of PKC-theta in the development and function of natural regulatory T cells.," *Mol. Immunol.*, vol. 46, no. 2, pp. 213–24, Dec. 2008.

[70] X. Wang *et al.*, "Effects of interleukin-6, leukemia inhibitory factor, and ciliary neurotrophic factor on the proliferation and differentiation of adult human myoblasts.," *Cell. Mol. Neurobiol.*, vol. 28, no. 1, pp. 113–24, Jan. 2008.

[71] A. Zanin-Zhorov *et al.*, "Protein kinase C-theta mediates

negative feedback on regulatory T cell function.," *Science*, vol. 328, no. 5976, pp. 372–6, Apr. 2010.

[72] B. Lozanoska-Ochser *et al.*, "Targeting early PKCθ-dependent T-cell infiltration of dystrophic muscle reduces disease severity in a mouse model of muscular dystrophy," *J. Pathol.*, vol. 244, no. 3, pp. 323–333, Mar. 2018.

[73] V. Marrocco *et al.*, "Pharmacological Inhibition of PKCθ Counteracts Muscle Disease in a Mouse Model of Duchenne Muscular Dystrophy.," *EBioMedicine*, vol. 16, pp. 150–161, Feb. 2017.

[74] L. Madaro *et al.*, "PKC Theta Ablation Improves Healing in a Mouse Model of Muscular Dystrophy," *PLoS One*, vol. 7, no. 2, p. e31515, Feb. 2012.

[75] C. F. Bentzinger, Y. X. Wang, N. A. Dumont, and M. A. Rudnicki, "Cellular dynamics in the muscle satellite cell niche," *EMBO Rep.*, vol. 14, no. 12, pp. 1062–1072, Dec. 2013.

[76] L. Machado *et al.*, "In Situ Fixation Redefines Quiescence and Early Activation of Skeletal Muscle Stem Cells," *Cell Rep.*, vol. 21, no. 7, pp. 1982–1993, Nov. 2017.

[77] E. J. Quann, X. Liu, G. Altan-Bonnet, and M. Huse, "A cascade of protein kinase C isozymes promotes cytoskeletal polarization in T cells.," *Nat. Immunol.*, vol. 12, no. 7, pp. 647–54, May 2011.

[78] V. Marrocco, P. Fiore, L. Madaro, A. Crupi, B. Lozanoska-Ochser, and M. Bouché, "Targeting PKCθ in skeletal muscle and muscle diseases: good or bad?: Table 1," *Biochem. Soc. Trans.*, vol. 42, no. 6, pp. 1550–1555, Dec. 2014.

[79] E. L. Sutcliffe *et al.*, "Chromatin-Associated Protein Kinase C-θ Regulates an Inducible Gene Expression Program and MicroRNAs in Human T Lymphocytes," *Mol. Cell*, vol. 41, no. 6, pp. 704–719, Mar. 2011.

[80] Y. Terada, M. Tatsuka, F. Suzuki, Y. Yasuda, S. Fujita, and M. Otsu, "AIM-1: a mammalian midbody-associated protein

required for cytokinesis.," *EMBO J.*, vol. 17, no. 3, pp. 667–76, Feb. 1998.

[81] M. Passalacqua, M. Patrone, B. Sparatore, E. Melloni, and S. Pontremoli, "Protein kinase C-theta is specifically localized on centrosomes and kinetochores in mitotic cells.," *Biochem. J.*, vol. 337 (Pt 1), pp. 113–8, Jan. 1999.

[82] L. Madaro *et al.*, "PKCθ signaling is required for myoblast fusion by regulating the expression of caveolin-3 and β1D integrin upstream focal adhesion kinase," *Mol. Biol. Cell*, vol. 22, no. 8, pp. 1409–1419, Apr. 2011.

[83] J. L. Watkins, K. T. Lewandowski, S. E. M. Meek, P. Storz, A. Toker, and H. Piwnica-Worms, "Phosphorylation of the Par-1 polarity kinase by protein kinase D regulates 14-3-3 binding and membrane association," *Proc. Natl. Acad. Sci.*, vol. 105, no. 47, pp. 18378–18383, Nov. 2008.

[84] M. Kwon *et al.*, "Mechanisms to suppress multipolar divisions in cancer cells with extra centrosomes," *Genes Dev.*, vol. 22, no. 16, pp. 2189–2203, Aug. 2008.

[85] A. S. Brack and P. Muñoz-Cánoves, "The ins and outs of muscle stem cell aging.," *Skelet. Muscle*, vol. 6, p. 1, 2016.

[86] J. D. Bernet, J. D. Doles, J. K. Hall, K. Kelly Tanaka, T. A. Carter, and B. B. Olwin, "p38 MAPK signaling underlies a cell-autonomous loss of stem cell self-renewal in skeletal muscle of aged mice.," *Nat. Med.*, vol. 20, no. 3, pp. 265–71, Mar. 2014.

7. LIST OF PUBLICATIONS

[1] **Benedetti A.,** Fiore P., Di Maggio R., Lozanoska-Ochser B. and Bouchè M. Inhibition of PKCθ stimulates satellite cell self-renewal. *Manuscript in preparation.*

[2] Fiore P., **Benedetti A.,** Sandonà M., Madaro L., De Bardi M., Saccone V., Puri PL., Gargioli C., Lozanoska-Ochser B. and Bouchè M. Lack of PKCθ promotes regenerative ability of muscle stem cells in chronic muscle injury. (2020) Int. J. Mol. Sci. *Accepted*. (Impact Factor 2018: 4.183).

[3] Rizzo G., Di Maggio R., **Benedetti A.**, Morroni J., Bouche M., and Lozanoska-Ochser B. Splenic Ly6Chi monocytes are critical players in dystrophic muscle injury and repair. (2019) JCI Insight Dec 24 [Epub ahead of print]. (Impact Factor 2018: 6.014).

[4] Renzini A., **Benedetti A.**, Bouche M., Silvestroni L., Adamo S., & Moresi V. Culture conditions influence satellite cell activation and survival of single myofibers. (2018) Eur. J. Transl. Myol., 28(2).

[5] Lozanoska-Ochser B., **Benedetti A.**, Rizzo G., Marrocco V., Di Maggio R., Fiore P. and Bouche M. 2018, Targeting early PKCθ-dependent T-cell infiltration of dystrophic muscle reduces disease severity in a mouse model of muscular dystrophy. (2018) J. Pathol., 244: 323-333. (Impact Factor 2017: 6.253).

[6] Marrocco V., Fiore P., **Benedetti A.**, Pisu S., Rizzuto E., MusaroA., Madaro L., Lozanoska-Ochser B., Bouche M. Pharmacological inhibition of PKCθ counteracts muscle disease in a mouse model of Duchenne muscular dystrophy. (2017) EBioMedicine, 16: 150-161. (Impact Factor 2018-19: 6.680).

ACKNOWLEDGEMENTS

I want to express my gratitude to my supervisor Marina Bouchè and Biliana for their guidance and support during my PhD. Your suggestions and constructive criticisms motivated me and helped me to grow as a student.

A special thanks to all my friends: Rosanna, Piera, Pino, Rita, Claudia, Erica, Ernestina, Alessandra, Jairo, and Cesar. Thank you for all the fun we had! I couldn't ask for better friends to share this experience.

I also thank my labmates for their help and suggestions: Claudio, Jacopo, Luca, Daisy, and Francesco. It has been a pleasure to work with you.

Finally, I thank my family and Sergio for their constant support and for encouraging me whenever I needed it.